NSWC TR 80-487

MACH 10/14 OPERATIONS IN THE NSWC HYPERVELOCITY WIND TUNNEL NO. 9 (VERTICAL HEATER VESSEL LEG)

BY ROBERT A. KAVETSKY

STRATEGIC SYSTEMS DEPARTMENT

16 JULY 1982

NAVAL SURFACE WEAPONS CENTER

Dahlgren, Virginia 22448 • Silver Spring, Maryland 20910

UNCLASSIFIED

SECURITY CLASSIFICATION OF THIS PAGE *(When Data Entered)*

REPORT DOCUMENTATION PAGE		READ INSTRUCTIONS BEFORE COMPLETING FORM
1. REPORT NUMBER NSWC TR 80-487	2. GOVT ACCESSION NO. AD-A132 235	3. RECIPIENT'S CATALOG NUMBER
4. TITLE *(and Subtitle)* MACH 10/14 OPERATIONS IN THE NSWC HYPERVELOCITY WIND TUNNEL NO. 9 (VERTICAL HEATER VESSEL LEG)		5. TYPE OF REPORT & PERIOD COVERED Final 6. PERFORMING ORG. REPORT NUMBER
7. AUTHOR(s) Robert A. Kavetsky		8. CONTRACT OR GRANT NUMBER(s)
9. PERFORMING ORGANIZATION NAME AND ADDRESS Naval Surface Weapons Center (Code K23) White Oak Laboratory Silver Spring, MD 20910		10. PROGRAM ELEMENT, PROJECT, TASK AREA & WORK UNIT NUMBERS 17X4912.3789, 0, 0, 0
11. CONTROLLING OFFICE NAME AND ADDRESS		12. REPORT DATE 16 July 1982 13. NUMBER OF PAGES 83
14. MONITORING AGENCY NAME & ADDRESS*(if different from Controlling Office)*		15. SECURITY CLASS. *(of this report)* UNCLASSIFIED 15a. DECLASSIFICATION/DOWNGRADING SCHEDULE

16. DISTRIBUTION STATEMENT *(of this Report)*
Approved for public release, distribution unlimited.

17. DISTRIBUTION STATEMENT *(of the abstract entered in Block 20, if different from Report)*

18. SUPPLEMENTARY NOTES

19. KEY WORDS *(Continue on reverse side if necessary and identify by block number)*

Hypervelocity Facility	Structural Analyses
Vertical Heater Vessel	Expansion Wave
Gas Dynamics	Flow Restrictor
Run Time	Particle Separator
Reynolds Number	Insulation Liners

20. ABSTRACT *(Continue on reverse side if necessary and identify by block number)*

The original design of the Tunnel No. 9 Hypervelocity Facility called for three distinct Mach number capabilities; namely Mach-10, Mach-15, and Mach-20. The Mach-15 (now Mach-14) and Mach-10 legs are operational. However, problems have been encountered in using a horizontal heater vessel to store hot test gas in the Mach-10 leg. A potential solution was to use the existing Mach-10 nozzle in combination with the Mach-14 heater vessel. After several design changes were implemented to mate the Mach-10 nozzle with the

DD FORM 1 JAN 73 1473 EDITION OF 1 NOV 65 IS OBSOLETE
S/N 0102-LF-014-6601

UNCLASSIFIED

SECURITY CLASSIFICATION OF THIS PAGE *(When Data Entered)*

20. Cont.

Mach-14 heater vessel, tunnel tests were conducted which demonstrated operational feasibility. However, unexpected high pressure drops resulted in a low Reynolds number. This report documents both Mach-10 and Mach-14 testing capabilities utilizing the Mach-14 heater vessel, and the analyses and testing on which the capabilities are based.

FOREWORD

The original design of the Hypervelocity Wind Tunnel No. 9 included two separate operational systems to obtain Mach-10 and Mach-14 test conditions. Severe thermal problems were encountered in using a horizontally positioned pressure vessel to contain hot test gas in the Mach-10 "leg," limiting test pressures, thus test Reynolds numbers. Subsequently, Mach-10 operations were moved to the Mach-14 leg, which employs a vertically positioned pressure vessel to store test gas, and which had been operated successfully for several years under much harsher (Mach-14) temperature and pressure conditions.

A series of wind tunnel runs demonstrated the feasibility of utilizing the Mach-14 leg for Mach-10 operations. The intent of this report is to document both Mach-10 and Mach-14 test capabilities in the Mach-14 leg.

O. F. BRAXTON
By direction

CONTENTS

ILLUSTRATIONS

TABLES

INTRODUCTION

The original design of the Tunnel No. 9 Hypervelocity Facility called for three distinct Mach number capabilities; namely Mach-10, Mach-15, and Mach-20. The Mach-15 leg (now Mach-14) and Mach-10 leg are operational. The Mach-20 leg is considered a future capability. As shown in Figure 1, the Mach-14 and Mach-20 legs utilize a vertically positioned gas heater vessel, while the Mach-10 leg employs a horizontally positioned vessel.

Problems have been encountered in using the horizontal heater vessel for Mach-10 operation. The major source of difficulty has been in trying to insulate the pressure vessel interior from the hot nitrogen test gas. As a result of this problem, the maximum heater pressure successfully obtained with the horizontal heater vessel thus far has been 7000 psi. The original design of the Mach-10 leg called for a maximum heater pressure capability of 15,000 psi and a predicted test Reynolds number of 15×10^6/ft. The 7000 psi pressure capability yielded a Reynolds number of approximately 8×10^6/ft; about half of what was desired. In addition, the horizontal heater vessel suffered from severe operability problems. The large temperature differences within the heater coupled with inherent design weaknesses led to breakdowns in internal components which made operations at Mach-10 less reliable and considerably more expensive than at Mach-14.

A potential solution to the operational problems noted above was to move Mach-10 operations to the Mach-14 leg. This would require using the Mach-10 nozzle in conjunction with the Mach-14 vertical heater vessel. This heater vessel has been operated successfully for several hundred tunnel runs, under test conditions (Mach-14 test gas temperature is 3100°F, pressure is 22,000 psi) much harsher than Mach-10 testing requires (Mach-10 test gas temperature is 1500°F). However, the mass flows at Mach-10 and high Reynolds numbers might cause greater stresses on internal components due to the rarefaction wave effects discussed later in this report. Also, due to heater vessel internal volume differences (30 ft^3 in the Mach-14 heater compared to 87 ft^3 in Mach-10 horizontal heater) valuable run time would be sacrificed.

A detailed engineering study indicated that it was technically feasible to use the Mach-14 heater/Mach-10 nozzle combination to achieve the high Reynolds numbers desired. The internal components of the heater could be redesigned to withstand the greater stresses predicted while providing a slightly larger

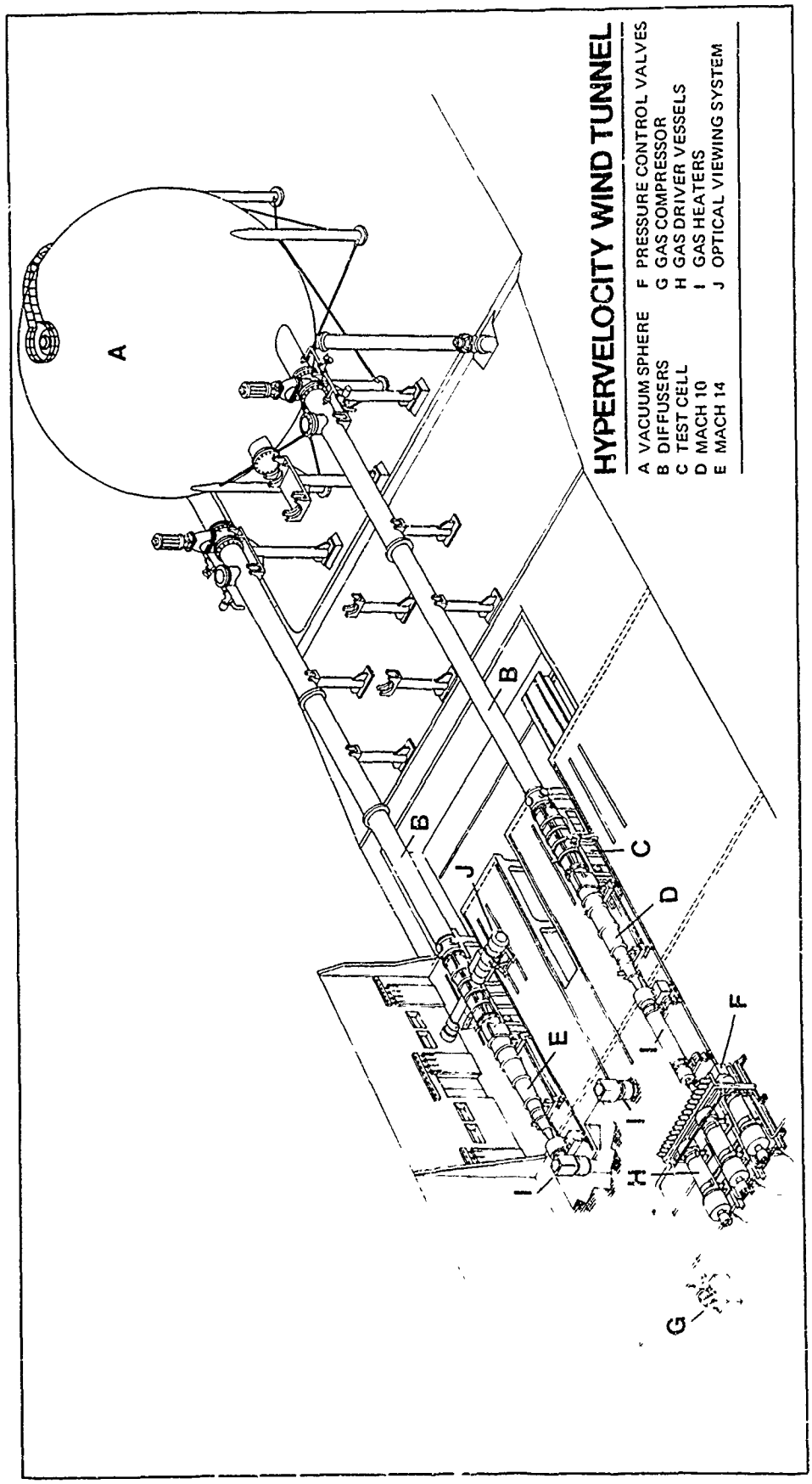

FIGURE 1 SCHEMATIC OF TUNNEL NO. 9 FACILITY

volume. The performance cost, assuming reliable operations could be achieved, would be a reduction in predicted run time from the 700 milliseconds attainable in the horizontal heater at Reynolds number of 8 x 10^6/ft to about 250 milliseconds at Reynolds number of 20 x 10^6/ft in the vertical heater. The shorter run time would still permit model pitch sweeps from -4 to +4 degrees angle of attack, which is the region of interest for stability testing of ballistic reentry bodies. The uncertainties in predicting such phenomena as the pressure drops through the system and the strength of the rarefaction wave at much higher pressures and mass flows led to a conservative, two-phase approach to implementing this solution. The first step involved redesign of the internal components coupled with the application of a "double sonic throat" technique in the flow as described below. The latter scheme promised the achievement of Reynolds numbers and run times comparable to those already achieved with the horizontal heater but with the reliability and cost achieved at Mach-14. The second phase would involve slowly increasing the nozzle supply pressure from 7,000 psi towards the 22,000 psi heater pressure limitation, thereby increasing the Reynolds number at the expense of run time. Even if the second phase uncovered intractable problems, the increased operability at Mach-10 and lower Reynolds numbers in the first phase was deemed a worthy goal.

After several design changes were implemented to mate the Mach-10 nozzle with the vertical heater vessel hardware, 18 tunnel runs were made in phase one. This test series successfully demonstrated the feasibility of the approach. The test results are documented in (Reference 1). However, due to larger than expected pressure drops through the "diaphragm section" (Figure 2), the highest Reynolds number achieved was 5.6 x 10^6/ft, 30% less than predicted. The purpose of this report is to present the capabilities of both Mach-14 and Mach-10 operations following the completion of phase one, and to document the analyses and testing on which these capabilities are based.

TUNNEL OPERATION DESCRIPTION

Figure 2 is a schematic of the vertical heater vessel and flow passage arrangement.

In operation, nitrogen at room temperature is used to fill the heater to a pressure on the order of one-quarter of the desired test pressure. Electrical power (up to a megawatt) is then applied to heat the gas and, at the same time, pressurize it at a constant volume. The nitrogen is contained in the heater by a dual diaphragm assembly as shown. These are ruptured to start a run by pressurizing the inter-diaphragm volume. The hot test gas is driven at a constant pressure through the nozzle throat by cold nitrogen initially stored at a higher pressure in the driver vessels. The flow of this gas is modulated by servo control values installed as shown. An inlet manifold upstream of the valves distributes the flow from the driver vessels to the inlets of the valves. An outlet manifold downstream of the valves directs the flow to the heater inlet

---

[1]Ragsdale, W. C., "Pershing II Static Stability and Pressure Test in the NSWC Hypervelocity Wind Tunnel," NSWC MP 80-493, Oct 1980.

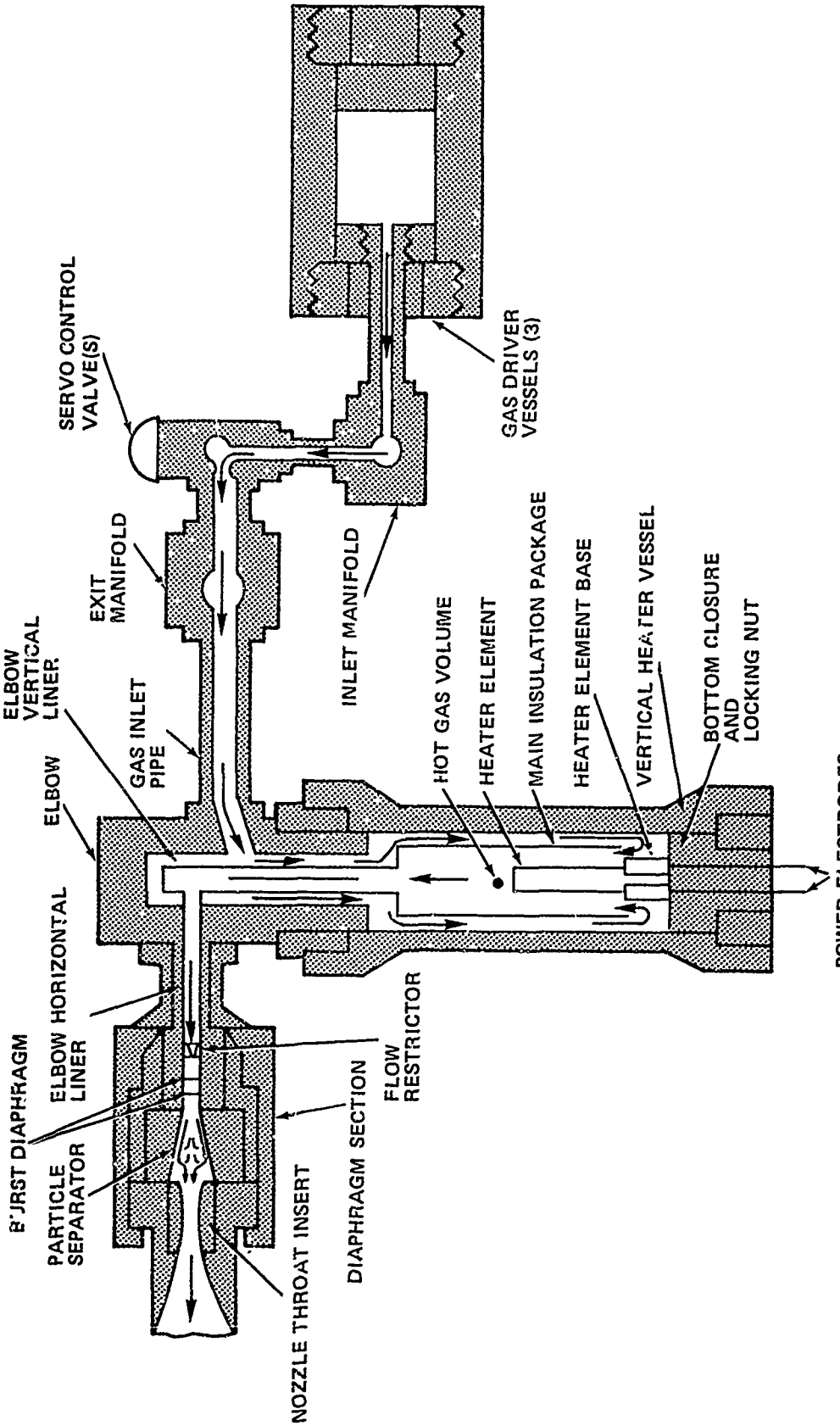

FIGURE 2 TUNNEL 9 VERTICAL HEATER AND FLOW PASSAGE ARRANGEMENT

pipe. The "cold" gas from the driver vessels proceeds from the heater inlet pipe, down through the annular gap between the main insulation liner outer jacket and the pressure vessel inner bore, turns 180°, and pushes the hot gas volume contained in the core of the vessel up, in a piston-like fashion, through the "elbow" and diaphragm sections.

A typical Mach-14 run, from diaphragm burst to flow breakdown lasts about 1.3 seconds, during which approximately .8 seconds of "good" flow is obtained. A tunnel run can be broken down into several regimes, as depicted in Figure 3. After diaphragm burst, the tunnel requires .5 seconds to warm up. Following the warmup period, "good" flow is established and data is taken (good flow is defined as condensation-free flow in the test cell). When all of the hot test gas has been expelled from the heater, the tunnel test is complete.

From an operability viewpoint, two portions of the tunnel run are of particular interest; the initial transient condition which occurs during the first 100 msec after diaphragm burst, and the steady-state regime during which "good" flow is established and data taken.

The transient period is characterized by a rarefaction wave, resulting from diaphragm burst, which moves back into the heater. The pressure oscillations experienced by various heater vessel internal components can be of a large magnitude. The survival of the various heater insulation packages (shown in Figure 2), which are exposed to this phenomenon, is of utmost importance during the transient period.

The steady-state flow regime is characterized by uniform flow through the vertical flow passage. Primary concerns during this time are pressure drops across the insulation packages (arising from flow friction losses in annular gaps around the insulations liners), and pressure drops across various diaphragm area components. At the end of the steady-state regime, the control valves close, shutting off the supply of driver vessel gas, and thus allowing the heater vessel to depressurize. If the control valves were to slam shut at the end of a run due to a malfunction, the depressurization of the heater vessel would be more severe, placing additional loads on heater vessel internal components.

Most of the Hypervelocity Facility's operability limitations can be attributed to concerns about the ability of tunnel hardware to withstand the extreme pressures and temperatures encountered during the two phases of a tunnel run noted above. Thus, a major portion of this report will deal with tunnel operations during the transient and steady-state regimes, as they will henceforth be called.

MACH-14 OPERATION

Table 1 contains operating characteristics and capabilities of the present Mach-14 assembly. Typically the Mach-14 leg operates with a heater pressure of 22,000 psi and a driver vessel pressure of 32,000 psi. The heater gas temperature is 3100°F and the driver gas temperature 300°F.

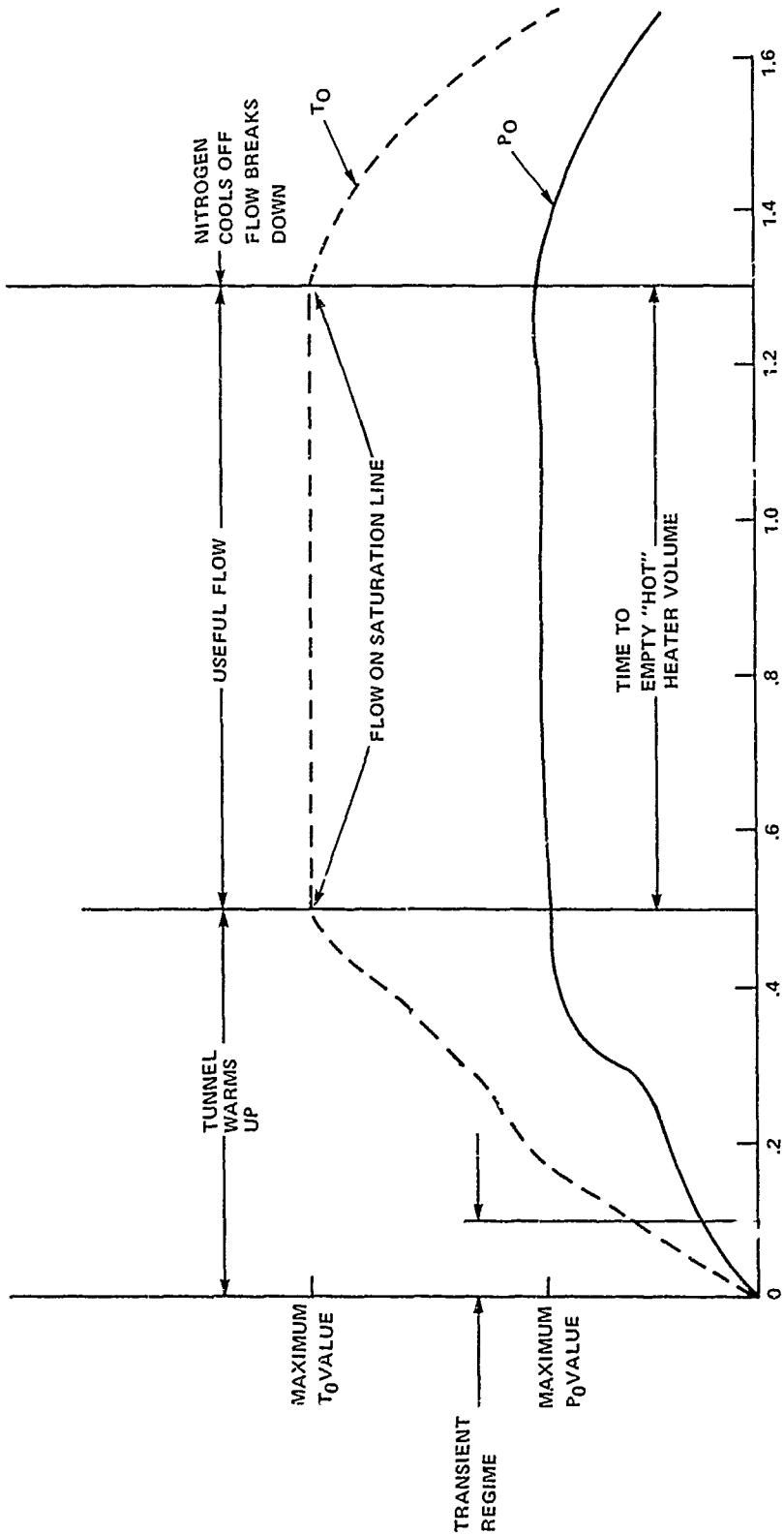

FIGURE 3 TYPICAL TUNNEL RUN

TABLE 1 TUNNEL 9 OPERATING CHARACTERISTICS

FLUID-NITROGEN
TEST SECTION-5 FOOT DIAMETER

MACH NUMBER	14	10
MAXIMUM HEATER GAS PRESSURE (psi)	22,000	22,000
MAXIMUM HEATER GAS TEMPERATURE (°F)	3,100	1,500
MAXIMUM SUPPLY PRESSURE (psi)	20,000	5,000
MAXIMUM REYNOLDS NUMBER (Ft^{-1})	4.2×10^6	5.6×10^6
TOTAL RUN TIME (AT MAX. REYNOLDS NO.) (Sec.)	1.2 –1.4	1.2 –1.4
USEFUL RUN TIME (Sec)	.5 –.9	.5 –2.0
CORE DIAMETER (inches)	30	36

TRANSIENT REGIME. As noted on Figure 3, the transient period lasts approximately 100 msec and is characterized by a rarefaction wave, resulting from diaphragm burst, which moves back into the heater. Figure 4 depicts the wave, in several locations in the vertical flow passage.

From a structural viewpoint, an oscillating pressure load is placed on the insulation packages due to the low pressure region of gas behind the wave, acting on the inside of the liners, and a high pressure region of gas acting on the outside of the liners. The need for a "flow restrictor" to mitigate the magnitude of the wave was recognized early during the shakedown phase of the facility. As shown in Figure 2, this flow restrictor is part of the diaphragm section of the tunnel.

To determine the strength of the wave moving back into the heater, crystal gage pressure transducers were mounted in the top and bottom of the heater vessel during several "cold" shakedown runs. Figure 5 is a graph of the measured pressure oscillations. As Jack Hill, the Division's Chief Aerodynamicist observed; "At the top of the heater there is a damped oscillation with a well defined frequency. At the bottom of the heater there is an initial pulse followed by secondary pulses of lesser amplitude. Also apparent, on a slower time scale, is the initial drop in heater pressure before the servo valves act to control it. It became apparent that the rarefaction wave moving into the heater was similar to that in a Ludweig tube."[2]

To calculate the strength of the expansion wave the small-disturbance formula for isentropic waves was used,

$$\Delta P = \rho_H a_H u \tag{1}$$

As in the Ludweig tube, the value u in a duct of cross-sectional area A is obtained from the equation,

$$\rho_H u A = \rho^* a^* A_R = k_n \rho_H a_H A_R \tag{2}$$

since $a_H^2 = \gamma P_H/\rho_H$, equation (1) becomes;

$$\Delta p/P_H = \gamma k_n \left(\frac{A_R}{A}\right) \tag{3}$$

This result (Equation 3) is shown as the solid curve in Figure 6 for the horizontal elbow section, in Figure 7 for the vertical elbow section and in Figure 8 for the main heater section. As noted on Figures 6, 7, and 8, the restrictor Area - $A_R = 1.4A^*$. This A_R, based on seven - .46 inch diameter flow restrictor holes, has been found to be the minimum A_R for which good flow recovery is obtainable. In all cases, the value plotted is $2\Delta p$ since the data represents the sum of an incident and reflected wave.

---

[2]Hill, Jacques A. F., "Initial Operation of the NOL Hypervelocity Tunnel," AIAA Paper 74-608, Jul 1974.

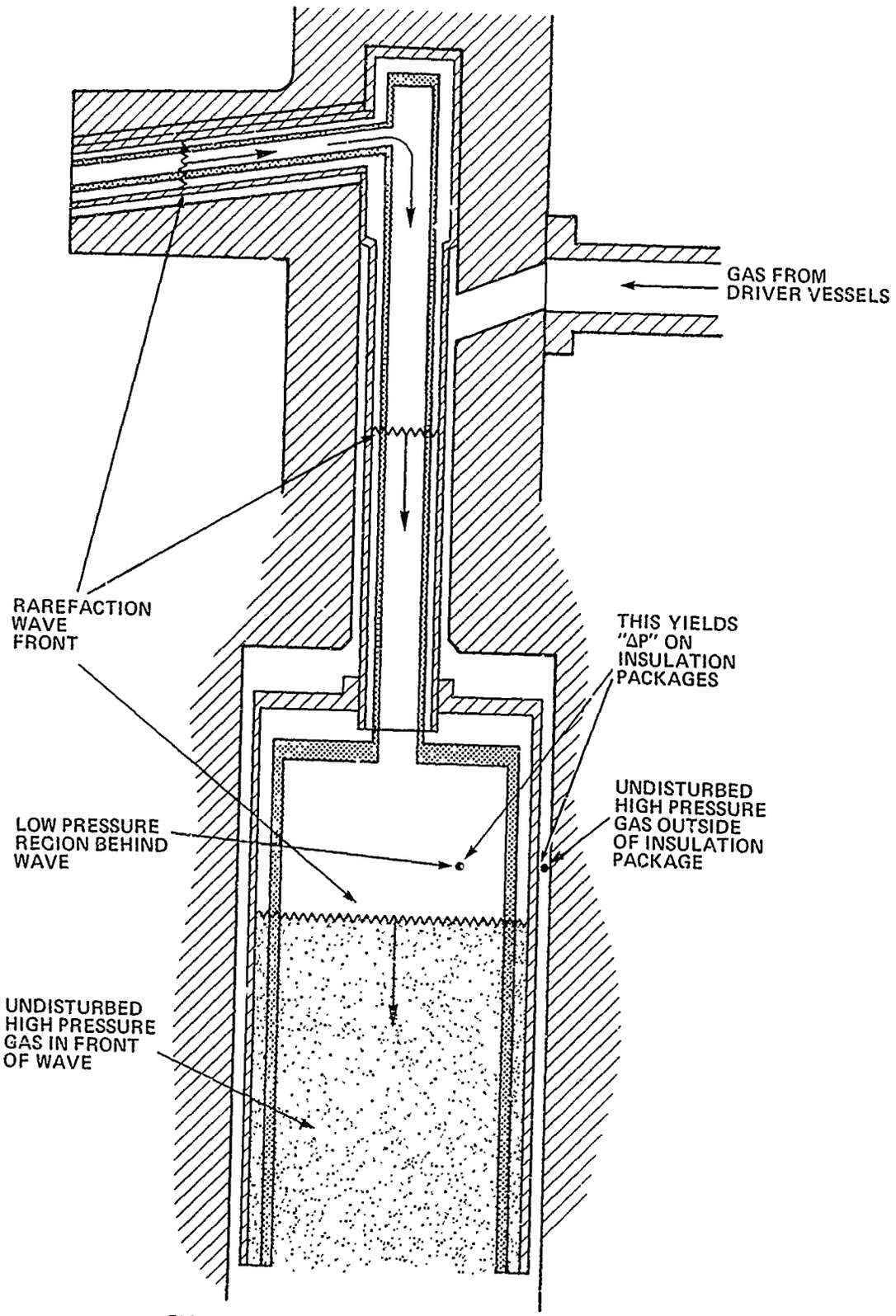

FIGURE 4 RAREFACTION WAVE MOVING BACK THRU VERTICAL FLOW PASSAGE

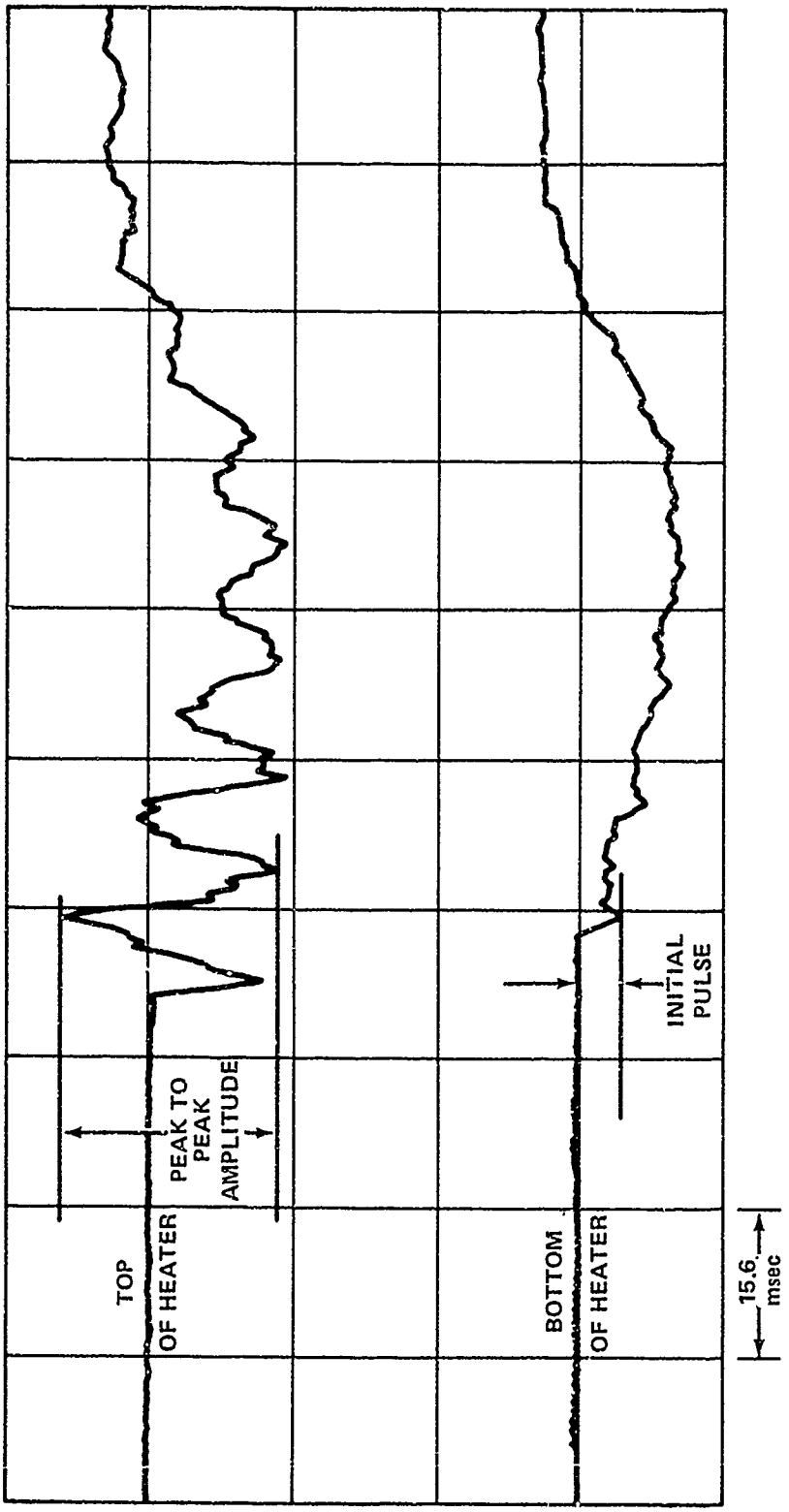

FIGURE 5 MEASURED PRESSURE OSCILLATIONS IN HEATER

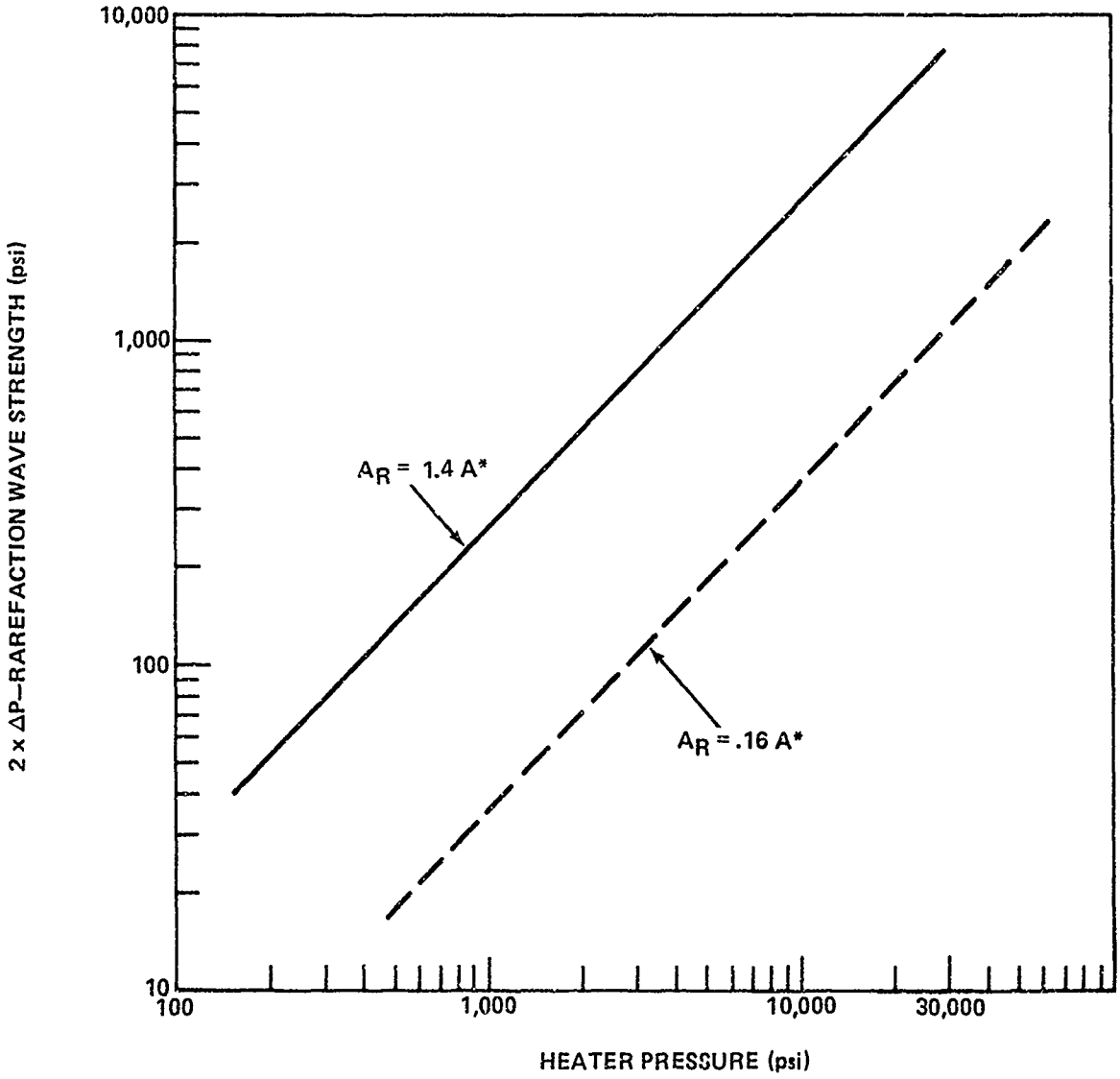

FIGURE 6 RAREFACTION WAVE STRENGTH VS HEATER PRESSURE, MACH-14 CONDITIONS, HORIZONTAL ELBOW

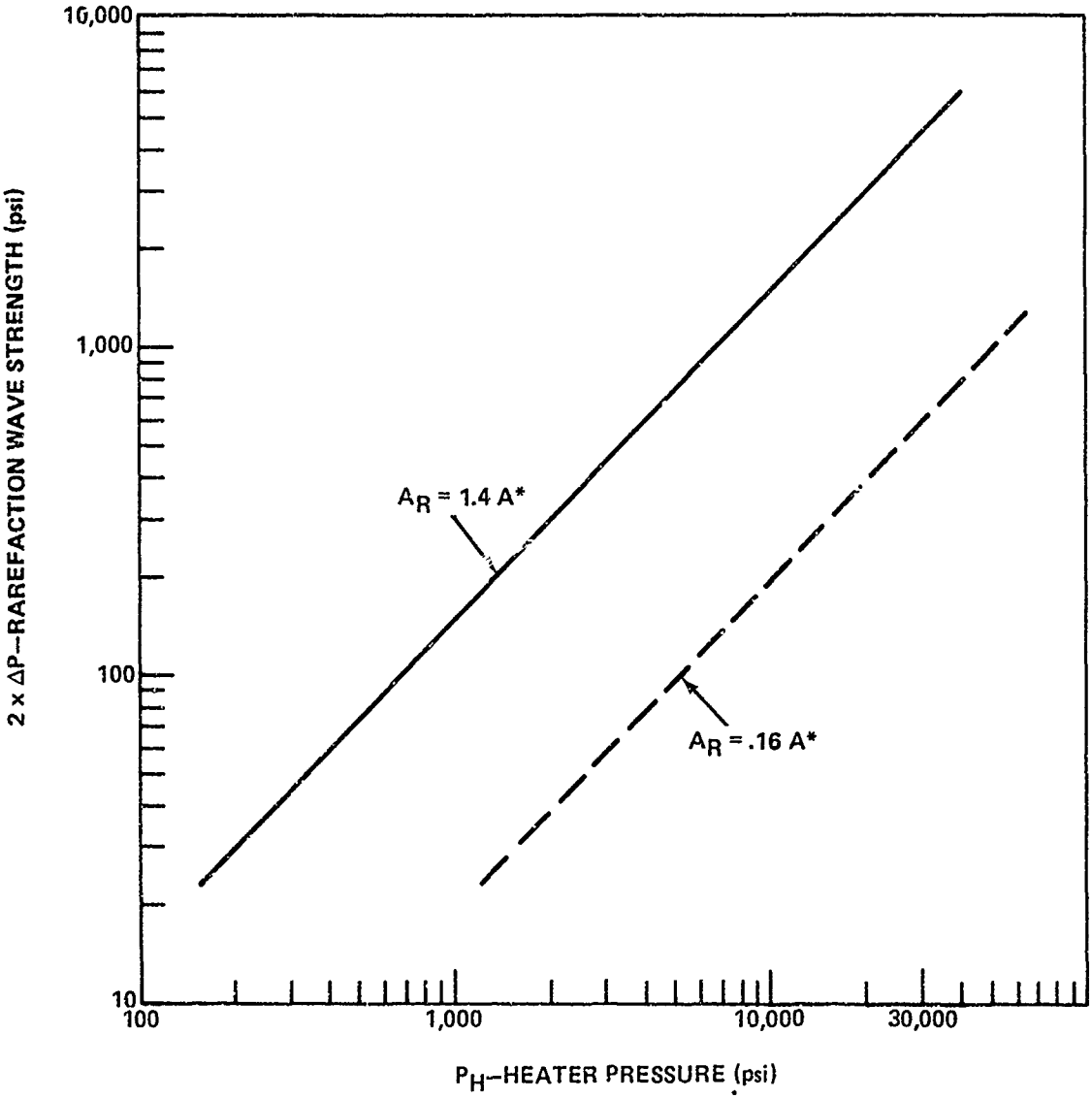

FIGURE 7 RAREFACTION WAVE STRENGTH VS HEATER PRESSURE, MACH-14 CONDITIONS, VERTICAL ELBOW

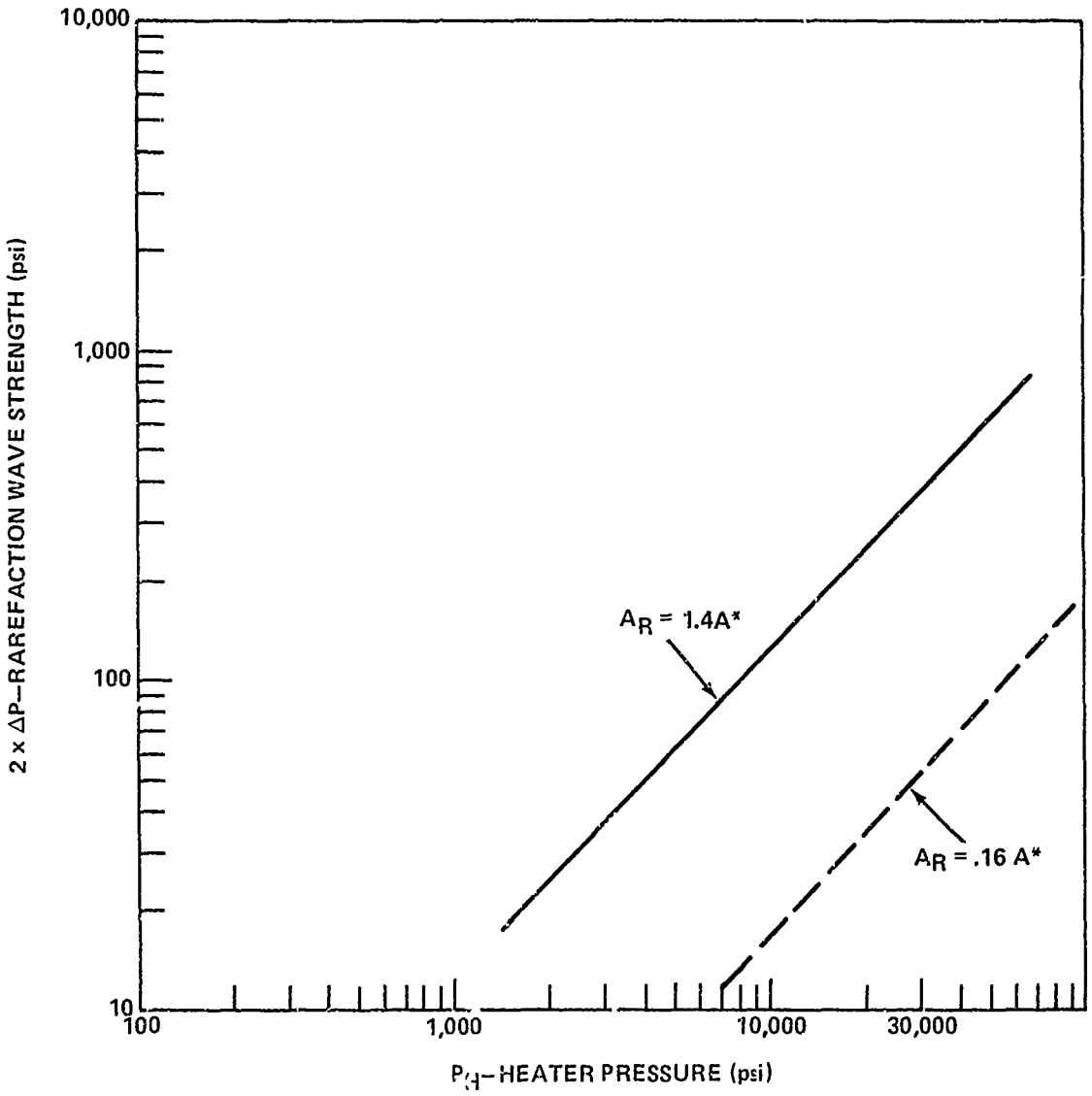

FIGURE 8 RAREFACTION WAVE STRENGTH VS HEATER PRESSURE, MACH 14 CONDITIONS, MAIN HEATER

During the shakedown phase of the Mach-14 leg it became apparent that it would be desirable to start a run with as small an initial A_R as possible, and then to "open up" A_R to some value larger than A^*. The solution was to employ an ablative insert in the flow restrictor design which would present a small initial A_R to the rarefaction wave, but would then open up to a larger A_R needed for good flow recovery. Several materials (Lucite, various Phenolics) were tested as ablators. The present material being used for all tunnel operations is "Delrin", an acetal resin. This material combines a high ablation rate with good mechanical strength. Now referring again to Figures 6, 7, and 8, the dashed curves correspond to the magnitude of the pressure wave based on an $A_R = .16$ in^2, which results from seven - .17 inch initial ablator hole diameters. Note the decrease in rarefaction wave strength in each area of the heater vessel when ablators are used. Figure 9 shows the present flow restrictor design, with ablator insert. The restrictor plate is fabricated from Columbium, a refractory metal with excellent high temperature strength properties.

Now having found the strength of the rarefaction wave in different areas of the heater vessel, determinations can be made as to whether various components (particularly the insulation packages) will retain their structural integrity.

Each insulation package consists of a perforated inner liner, a thickness of insulation material, and a solid outer shell. The rarefaction wave, in passing through the heater core, places the inner liners and outer jackets under an oscillating pressure load condition. Accordingly then, the buckling strength capabilities of the various components must be determined. Table 2 contains the results of calculations performed (in Appendix A) to determine static and dynamic buckling pressure capabilities of various internal components. Note the enhancement of buckling pressure capability when the applied load is impulsive in nature.

In examining the pressure traces shown in Figure 5, the question arises as to which buckling pressure value to use in comparison with rarefaction wave strength. An analysis of a liner which had previously failed indicated the external pressure applied was somewhere between the static and dynamic buckling capability of the liner. As a result of this analysis, and the pattern of the buckle observed in the failed liner, it was concluded that the load applied to the liner was quasi-static in nature. In order to be conservative then, the static buckling pressure was used for comparison purposes. Table 3 contains values of the magnitude of the rarefaction wave strength for the typical heater pressure of 22,000 psi. Two values, obtained from Figures 6, 7, and 8, are shown for each area of the heater. The "normal ablation" column of values refers to the situation in which the ablators function properly, i.e., the rarefaction wave magnitude is reduced by passing through the small initial ablator holes. Thus, these values were obtained from the dashed line on Figures 6, 7, and 8. The "ablator failure" column of values applies to any scenario in which the ablators might not function properly. Such a failure would occur if the ablators became too warm, lost strength, and sheared out instead of ablating out, thus exposing the insulation packages to a much stronger rarefaction wave.

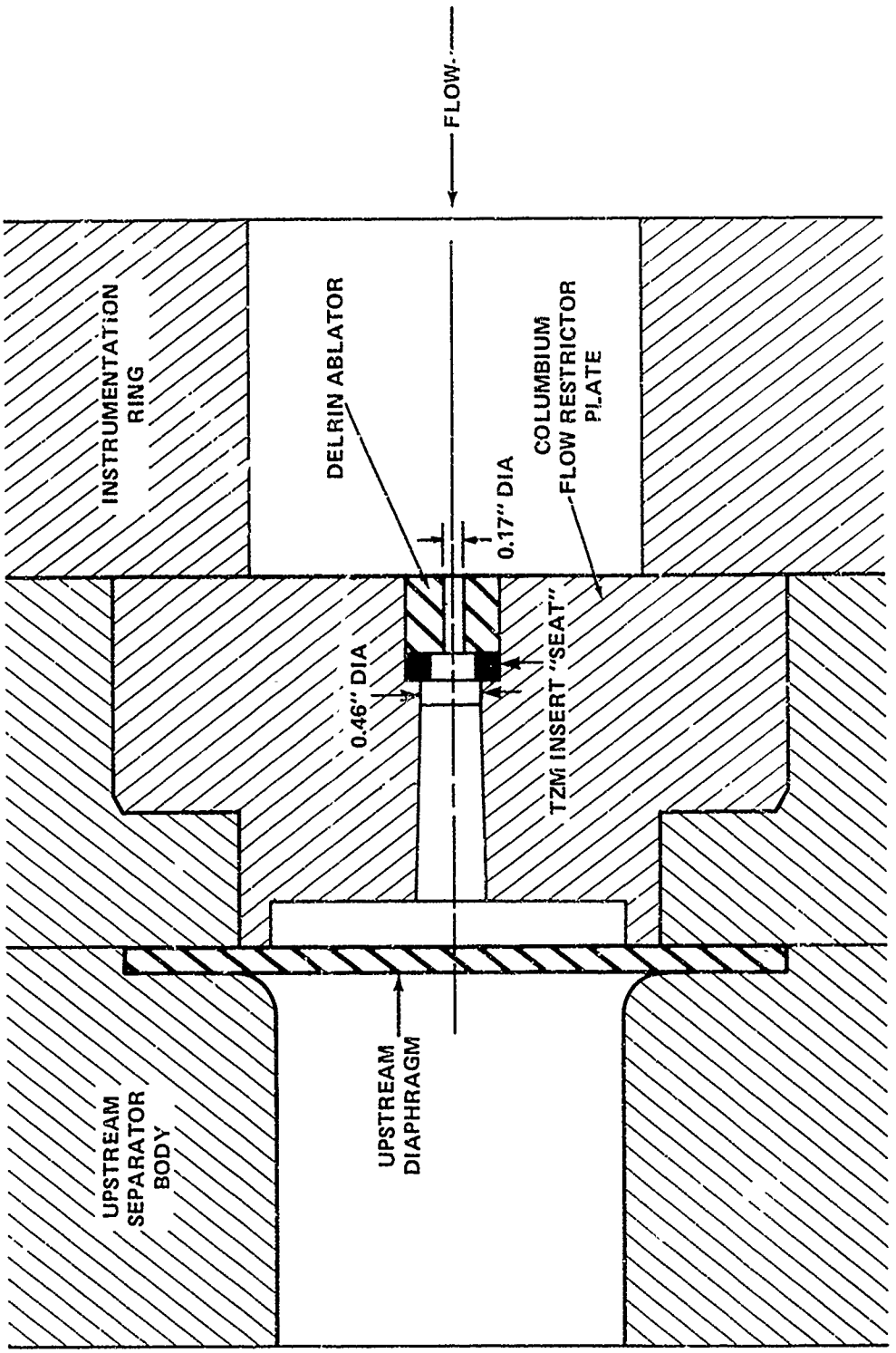

FIGURE 9 MACH–14 FLOW RESTRICTOR DESIGN

TABLE 2 LINER BUCKLING PRESSURE CAPABILITIES

	P_{CR}-STATIC BUCKLING PRESSURE (psi)	P_D-DYNAMIC BUCKLING PRESSURE (psi)
VERTICAL ELBOW OUTER JACKET	1400	4350
MAIN HEATER OUTER JACKET	1150	12,200
HORIZONTAL ELBOW OUTER JACKET	600	1440
VERTICAL ELBOW INNER LINER	150	1430
MAIN HEATER INNER LINER UPPER	120	1620
MAIN HEATER INNER LINER LOWER	160	1550
HORIZONTAL ELBOW INNER LINER	910	2680
TOP PLATE	690	–
SUPPORT RING	275	–

TABLE 3 STATIC BUCKLING CAPABILITY (P_{CR}) & EXPANSION WAVE STRENGTH

COMPONENT	P_{CR}	2ΔP NORMAL ABLATION (PSI)	2ΔP ABLATOR FAILURE (PSI)
VERTICAL ELBOW OUTER JACKET	1400	220	1600
MAIN HEATER OUTER JACKET	1150	30	210
HORIZONTAL ELBOW OUTER JACKET	600	440	3230
VERTICAL ELBOW INNER LINER	150	2	106
MAIN HEATER INNER LINER UPPER	120	.046	1.62
MAIN HEATER INNER LINER LOWER	160	.024	.82
HORIZONTAL ELBOW INNER LINER	910	18	966
TOP PLATE	690	30	210
SUPPORT RING	275	30	210

The values listed for the inner liners require additional explanation. The inner liners were initially perforated to facilitate the decompression of the porous insulation around the inner liner at the end of the tunnel run. However, the perforations also serve to lessen the severity of the rarefaction wave as it passes over the inner liners. The end result is that the inner liners "see" a much weaker loading condition than the outer jackets. Appendix B contains calculations demonstrating how the values listed in Table 3 were obtained.

Also shown in Table 3, for comparison purposes, are static buckling pressure capabilities for the liners. For the "with ablators" case, i.e., a normal strength rarefaction wave, all inner liners and outer jackets have an adequate buckling pressure capability. This is not the situation for the "without ablators" case. It appears that the vertical and horizontal elbow outer jackets and the horizontal elbow inner liner might not survive this "worst case" scenario. For this reason, much care and caution is taken to ensure successful ablator function during each tunnel run.

The top cover plate and support ring used with the main heater insulation package are also stressed by the rarefaction wave. The values listed in Table 3 for these components indicate they have adequate strength for a "normal" ablation situation.

The question arises as to why the liners were not designed to take the "without ablators" load. Simply put, the insulation packages were fabricated and installed before the rarefaction wave phenomena was identified as dangerous to the structural integrity of heater internals. Subsequent generations of heater internals should have the capability to withstand the worst case loading condition.

During the transient period the flow restrictor and particle separator experience a large initial pressure drop. However, the temperature of the gas passing through the flow restrictor is initially fairly low, (300°F), therefore, the "ligaments" (material between adjacent restrictor holes) retain their mechanical strength. Appendix C contains calculations indicating there is no structural problem with either the flow restrictor or particle separator during this time.

STEADY-STATE REGIME. When uniform flow is moving through the flow passage area, the outer jackets of the insulation packages are subjected to pressure drops occurring due to friction losses in the annular gaps between the outer jackets and the pressure vessel inner diameter. Figure 10 shows pressures at various locations during the steady-state flow condition. The calculations these pressures are based on are given in Appendix D. Table 4 lists the static buckling pressure capabilities of the outer jackets, which were described earlier. In addition, the steady-state pressure drops are listed. As can be seen from the values listed in Table 4, all the outer jackets have adequate buckling pressure capability to withstand this loading condition.

Near the end of the steady-state regime the control valves between the driver vessels and heater vessel close. During the initial operation of the tunnel there was a concern that if the control valves slammed shut, the volume of gas between the various inner liners and outer jackets would not have an adequate time to vent, thus putting a large external pressure load on the inner liners. As noted

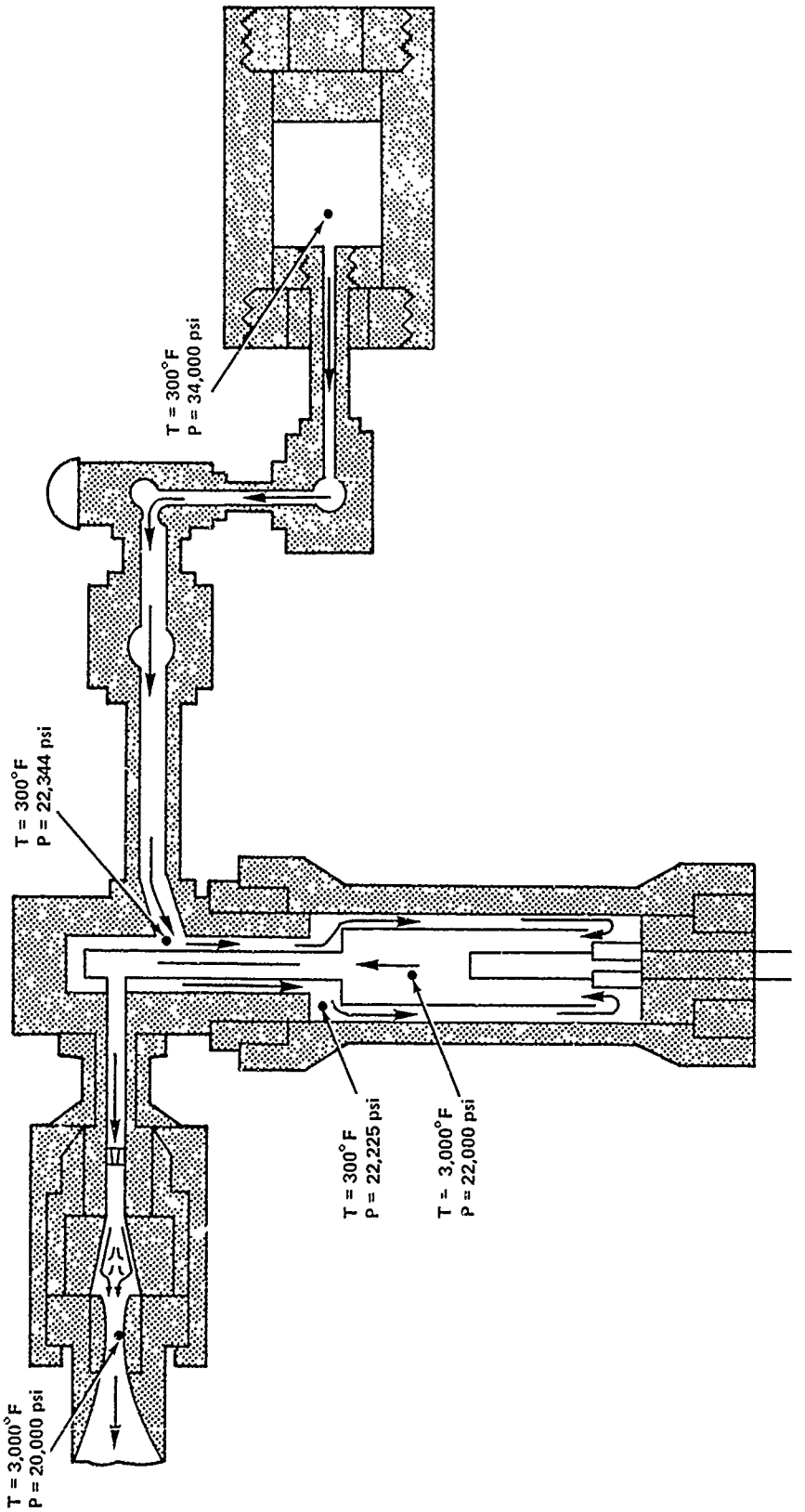

FIGURE 10 GAS CONDITIONS DURING STEADY-STATE FLOW REGIME (MACH-14)

TABLE 4 COMPARISON OF MACH-14 STEADY-STATE PRESSURE DROP & STATIC BUCKLING CAPABILITY

COMPONENT	STEADY-STATE PRESSURE DROP	P_{CR} – STATIC BUCKLING CAPABILITY
VERTICAL ELBOW OUTER JACKET	344	1400
MAIN HEATER OUTER JACKET	225	1150
HORIZONTAL ELBOW OUTER JACKET	344	600
TOP COVER PLATE	225	690
HEATER SUPPORT RING	225	275

earlier, the inner liners were perforated to preclude this possibility. Also since the initial shakedown, the control valve operation has been modified. The modification consisted of putting stops in the servo controller which limited the flow rate of hydraulic fluid to the control valve actuator, thus limiting valve speed. The end result of the modification was that the maximum valve stroke speed was reduced by a factor of seven, and that control valves "slamming shut" at the end of run would not be a problem.

During the steady-state regime, pressure drops occur across both the flow restrictor and particle separator. Figure 11 shows the pressure drops across the flow restrictor and particle separator vs time. In addition, the temperature rise of both components is shown. Heat transfer analyses indicated that the ligaments come up to nearly gas temperature very rapidly, as illustrated in Figure 11. The combined effect of pressure drop and temperature rise lead to concerns about the structural integrity of these components. Analyses of the particle separator and flow restrictor (Appendix C) indicate maximum pressure drop capabilities, at the maximum gas temperature, of 320 psi and 9240 psi respectively, for Mach-14 operation. In addition, all pressure containment components in the diaphragm area have been analyzed and approved for heater pressures up to 22,000 psi.[3]

MACH-10 OPERATION

OPERATIONAL BACKGROUND. As noted in the Introduction, Mach-10 operations utilizing the horizontal heater vessel were limited to a heater gas pressure of 7000 psi. Simply put, the problem was that the inner bore of the pressure vessel would reach its allowable temperature limit (500°F) before the test gas would reach desired conditions. Numerous schemes were employed to reduce or eliminate the problem, but it was finally decided that, short of major hardware changes, minimal increases in test Reynolds numbers were all that could be expected. In addition, operations in the horizontal heater vessel leg were limited to one run per day due to residual heat effects in the diaphragm area. Mach-14 operations typically allow for at least two runs per day, an important consideration to potential customers. The combined effect of both reduced pressure limits and lack of operability was to lead to the conclusion that Mach-10 testing using the horizontal heater vessel was not a viable option with respect to maintaining a state-of-the-art facility.

At this point investigations began, looking into the feasibility of using the Mach-14 heater vessel in conjunction with the Mach-10 nozzle (the same test cell would be used for both legs, regardless of location in the building). Insulating the hot gas from the pressure containment components and diaphragm section prior to diaphragm burst has not been a problem with the vertical vessel. In particular, the diaphragm area (including ablators) remains cool (100°F) during the heating of the test gas due to the unique 7° dogleg present in the vertical elbow (see Figure 2), thus preventing hot gas from moving down into the diaphragm area. In short, the vertical heater vessel had a proven operability record.

---

[3]ODAI Final Report No. 1270-8-79, "Hyper-Velocity Wind Tunnel Components Structural Evaluation," May 19?9.

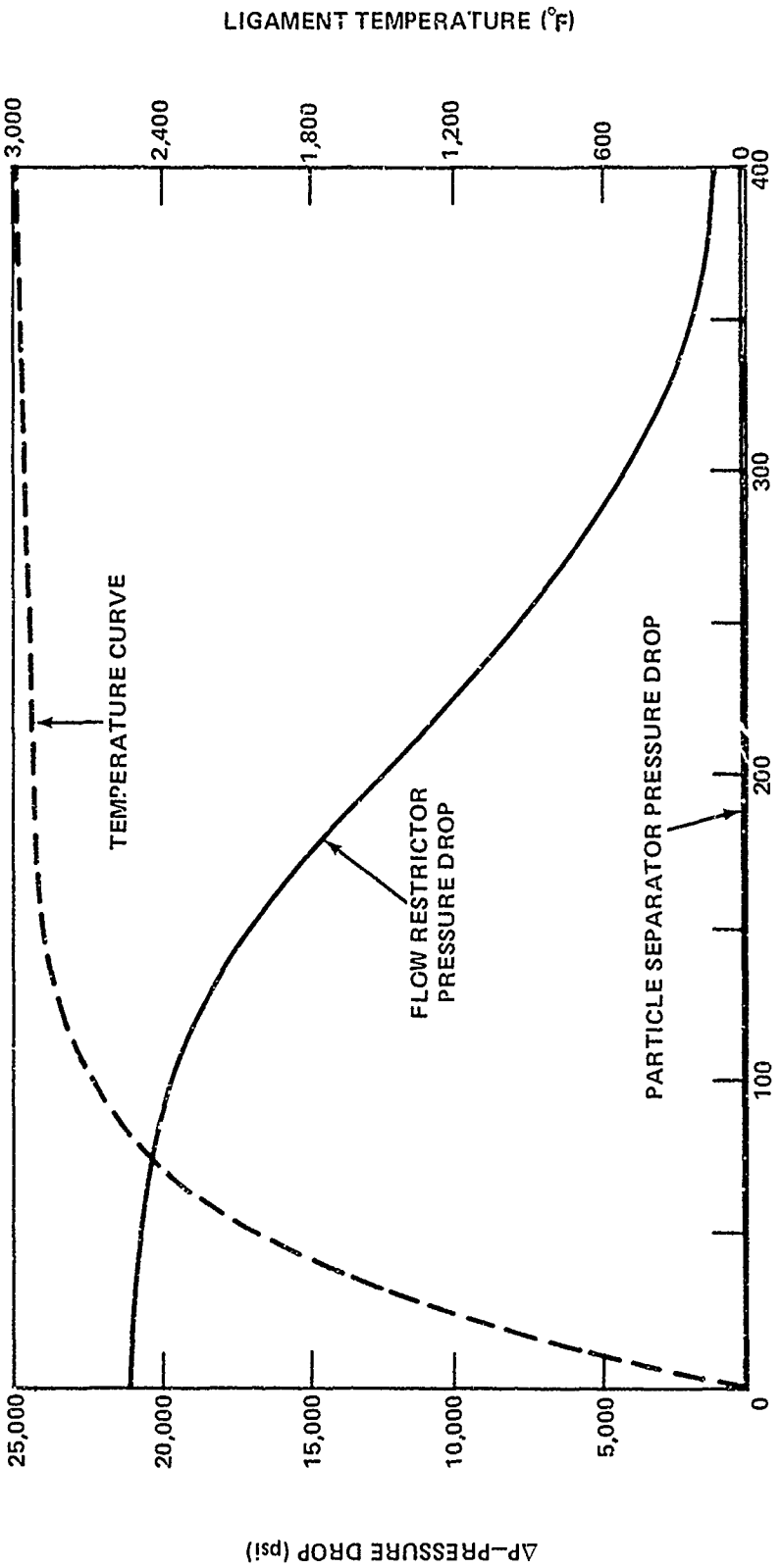

FIGURE 11 PRESSURE DROP(S) & TEMPERATURE RISE VS TIME FOR MACH-14 CONDITION

During the investigation, operational constraints were defined and analyzed as to potential effect on system performance. Table 5 contains a list of the constraints, reasons for the constraint, and system impact of the constraint. A few words are in order to further clarify the constraints put into effect.

Constraints 1, 4, and 5, as listed in Table 5 can be thought of as general facility limitations and are always in effect, no matter what the proposed configuration would ultimately turn out to be. Constraint 1 is based on the issue of overpressurization of the heater vessel if the control valves opened unexpectedly before a run, and gas from the driver vessels entered the heater vessel. Calculations have determined that the pressure in the heater vessel could rise to 28,500 psi, which is the maximum pressure limit as determined by finite element analyses and ASME code limitations.[3]

Constraint 4 was arrived at by considering both fatigue life implications on the driver vessels if the maximum pressure were allowed to rise to 40,000 psi, and the reliability of seals, compressors, etc. under this harsh pressure environment. As it turned out, this constraint did not limit system performance in any way, and in fact, a driver vessel pressure of 34,000 psi was more than adequate for the operational setup selected.

The constraint on heater element maximum current had been arrived at mainly thru operational experience. Problems had been encountered with heating elements cracking both during and after the heatup cycle. It was never determined whether material inconsistencies or too large a current was the culprit. However, since the time the maximum current level allowed was reduced from 6500 to 5500 amps, heater element operability problems have disappeared. Lastly, due to the lower gas temperature required for Mach-10 (1500°F) versus Mach-14 (3100°F), this constraint was not limiting. Heatup time for Mach-10 was estimated to be 10-12 minutes. In comparison, Mach-14 heatup time is 17-20 minutes.

To simplify the proposed operational setup, one of the initial ground rules was that existing Mach-14 insulation packages and heater element would be used. As it turned out, this decision essentially defined the maximum Reynolds number capability/run time curve for the vertical heater/Mach-10 nozzle combination. This decision is reflected in constraints 2, 3, and 4. If the heater vessel internal components were to remain the same, then the "hot" heater volume available (10.5 ft^3) would remain the same. Constraints 1 and 2, taken together, limit the mass of hot gas that can be expelled during a run, thus limiting the required driver vessel pressure to less than 40,000 psi.

Constraint 3 was placed on the system to ensure operability of both the new scheme and the existing Mach-14 testing capability. In other words, it was felt that, as long as the Mach-14 hardware was not subjected to loads greater than encountered in Mach-14 testing, then operability of the new configuration would be ensured. In addition, Mach-14 operations would not be adversely impacted.

As it turned out, constraint 3 fixed the maximum P_o, and therefore the maximum Reynolds number attainable, by limiting the flow restrictor open area to 1.16 in^2, the Mach-14 value.

---

[3]See footnote 3 on page 21.

TABLE 5 MACH -10 OPERATIONAL CONSTRAINTS

CONSTRAINT	RATIONALE	SYSTEM IMPACT
1. HEATER PRESSURE $\leq$22,000 psi	LIMIT BASED ON OVERSTRESS SITUATION IF CONTROL VALVE FAILURE OCCURS (OPEN)	PLACES UPPER BOUND ON REYNOLDS NO/RUN TIME TRADE OFF CURVE
2. "HOT" HEATER VOLUME $\simeq$10,5 ft^3	PHYSICAL CONSTRAINT IMPOSED BY SIZE OF VESSEL & INSULATION PACKAGES	LIMITS RUN TIME
3. RAREFACTION WAVE STRENGTH $\leq$ MACH-14 WAVE	MACH -14 HARDWARE HAS PROVEN STRUCTURAL CAPABILITLES TO A CERTAIN LEVEL. OPERABILITY NO PROBLEM AS LONG AS THIS LEVEL IS NOT EXCEEDED	LIMITS MAX REYNOLDS NUMBER ATTAINABLE
4. DRIVER GAS PRESSURE $\leq$ 40,000 psi	FATIGUE LIFE & OPERABILITY CONSIDERATIONS	NO EFFECT
5. MAX CURRENT IN HEATER ELEMENT $\leq$ 5500 AMPS	SAME AS 3	NO EFFECT

After having defined the constraints noted above, the following predictions concerning system performance were made;

a. The maximum test Reynolds number would be slightly less than that obtained in the horizontal heater vessel,

b. At the maximum Reynolds number, a run time of .3 seconds could be expected,

c. Due to area ratios involved between the flow restrictor and Mach-10 throat, the tunnel would operate as a double sonic throat (this prediction was based on calculations that indicated the pressure drop across the flow restrictor would be great enough to maintain choked flow thru the flow restrictor for all nozzle pressures allowed).

It was decided that the tradeoff in test Reynolds number capability was worth the potential increase in operability/reliability, and that the configuration should be tested.

Several design changes were required in the diaphragm area to mate Mach-10 hardware with Mach-14 hardware. Figure 12 contains schematics of the Mach-14 diaphragm section and the Mach-10/14 diaphragm section. Note that the existing Mach-14 flow restrictor, and Mach-10 particle separator are utilized in the new arrangement.

Subsequently, the vertical heater vessel/Mach-10 nozzle combination was successfully tested and did, in fact, demonstrate that the double sonic throat method is a viable concept for wind tunnel testing. Figure 13 is a graph of run time versus Reynolds number for the new combination. Both a test performance prediction curve, and an actual test performance curve are given. Several important points are contained in this figure. First, the maximum Reynolds number obtained was about 5.6×10^6/ft, which was 30% less than predicted. This was due to unexpectedly higher pressure drops existing across the flow restrictor. Second, if the maximum Reynolds number had been close to 8×10^6/ft, a severe run time penalty would have been imposed. The actual performance curve shown defines the Reynolds number - run time trade-off available to customers.

Returning to Table 1, note the operating characteristics and capabilities of the vertical heater vessel/Mach-10 nozzle combination. This combination operates typically with heater vessel pressure of 22,000 psi and a driver vessel pressure of 34,000 psi. The heater gas temperature is 1500°F and the driver gas temperature 300°F. Different P_o's (throat pressure) are obtained by placing various orifices in the flow restrictor (TZM "seats" shown in Figure 9). This results in a variable Reynolds number capability since Reynolds number is related to P_o.

TRANSIENT REGIME. The primary concern during this period, as in the Mach-14 case, is in keeping the rarefaction wave strength to an acceptable level. It can be shown that the transient condition for Mach-10 is less severe than the Mach-14 case, for a given heater pressure. Pertinent calculations are contained in Appendix E. The net result is that the rarefaction wave strength for Mach-10 operating conditions is 90% of the rarefaction wave strength for Mach-14 operating

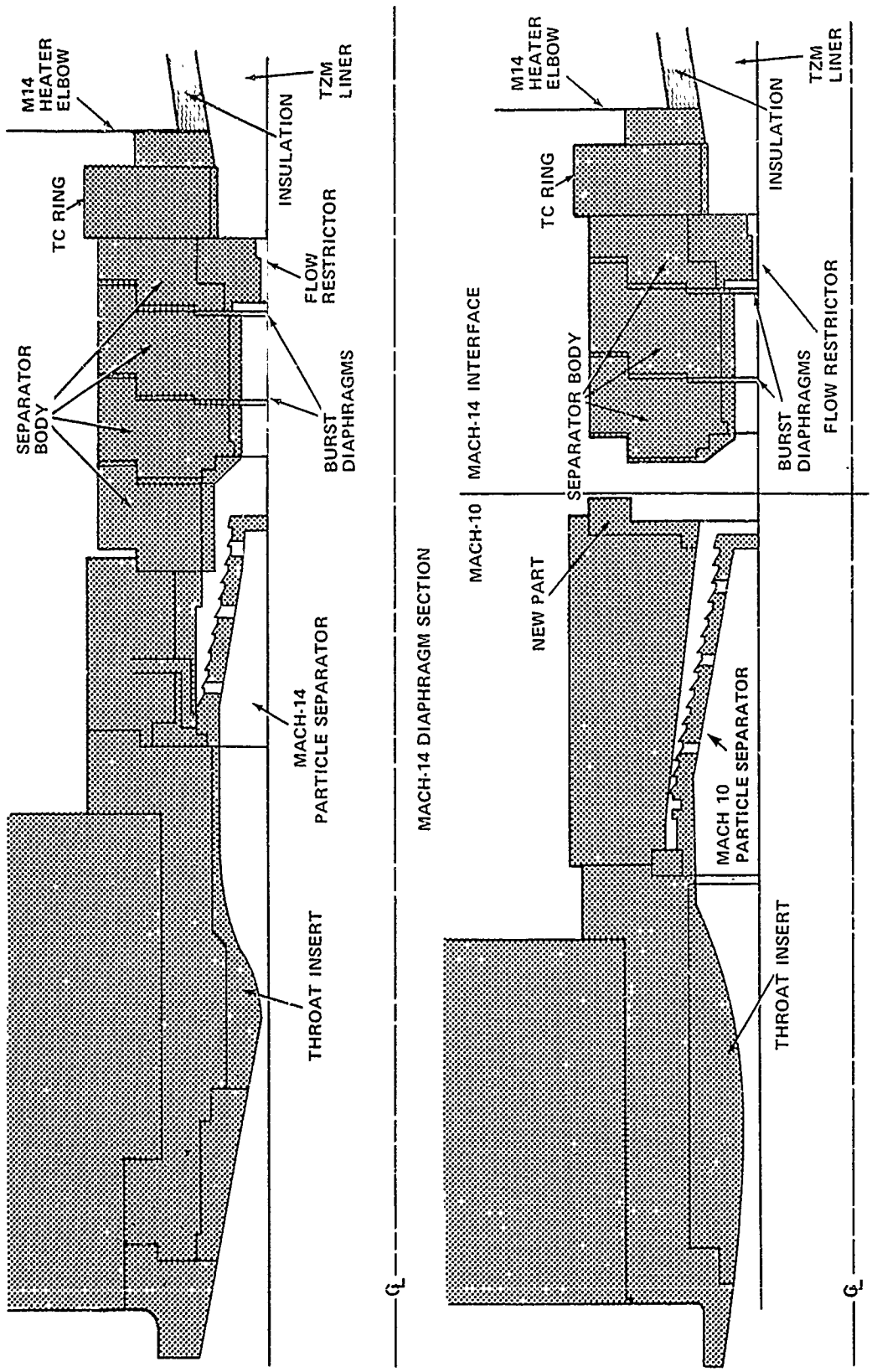

FIGURE 12 DIAPHRAGM AREAS, MACH-14 AND MACH 10/14

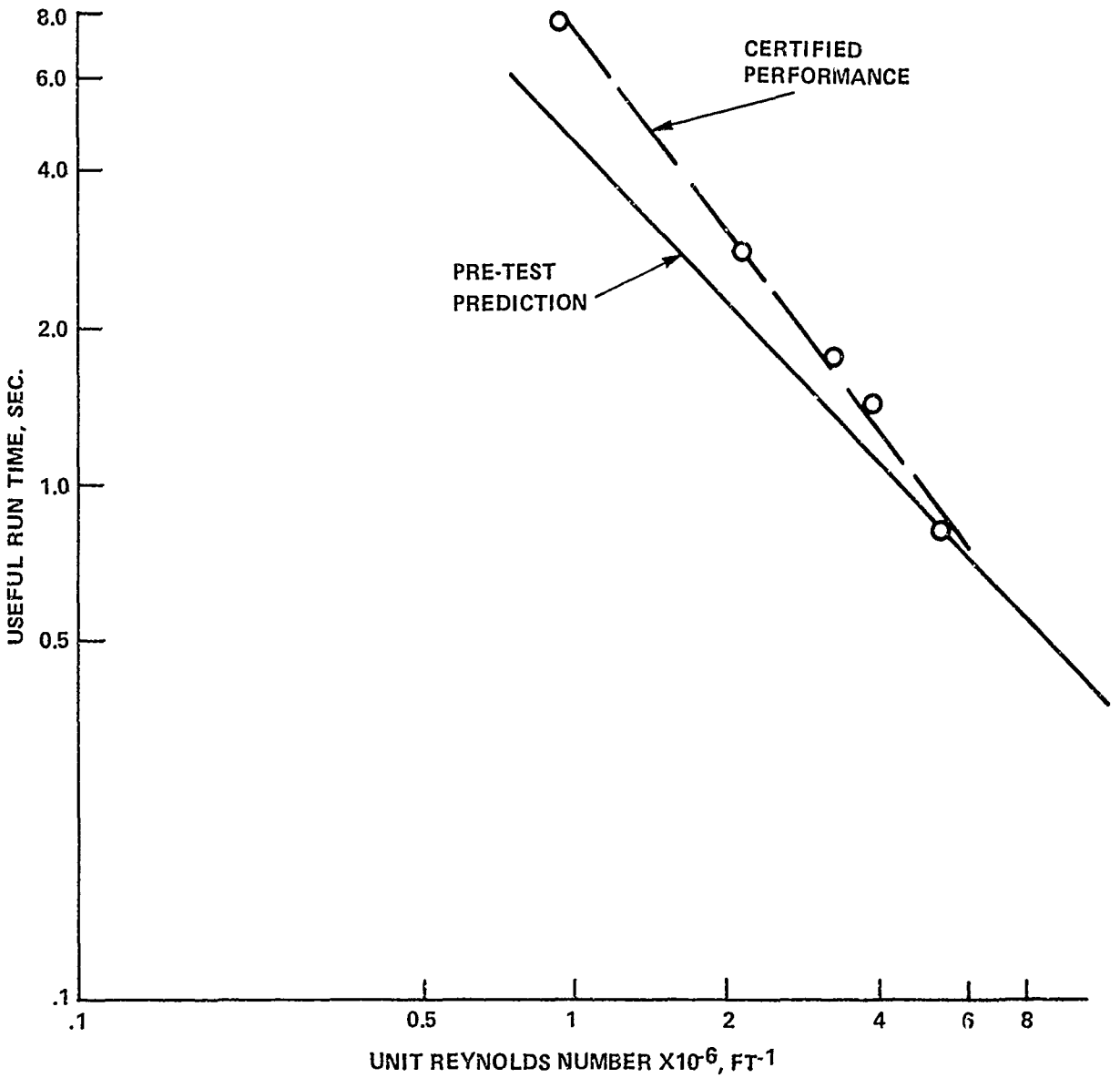

FIGURE 13 RUN TIME VERSUS UNIT REYNOLDS NUMBER

conditions. Therefore, the conclusions reached with regard to heater internals' survivability remain the same. To reiterate, all inner liners, outer jackets, the top cover plate and support ring will survive a normal ablation. In regards to the worst case, or without ablators scenario, the horizontal and vertical elbow outer jackets, horizontal elbow inner liner, and the heater support ring, appear to be structurally marginal.

As in the Mach-14 case, the flow restrictor and particle separator experience a large initial pressure drop. However, due to the low temperature of the gas (300°F) flowing through the diaphragm area at the time, calculations (contained in Appendix C) indicate no structural problem.

STEADY-STATE REGIME. As a result of the lower heater gas temperature required for Mach-10 operation, there is a greater mass of gas in the heater vessel. For a given pressure then, the mass flow rate throught the vertical flow passage must increase. Figure 14 notes pressure and temperature conditions of the nitrogen at various locations in the flow passage during the steady-state regime. Appendix D contains the calculations on which the values shown on Figure 14 are based. Table 6 contains the pressure drops obtained from the pressures shown in Figure 14. Also listed in Table 6 are the static buckling capabilities of the outer jackets. As can be seen, this mode of loading presents no threat to the structural integrity of the outer jackets, though more severe than the Mach-14 case (values shown in Table 4).

Calculations performed in Appendix E indicate the depressurization occurring at the end of a run is more severe in Mach-10 than in Mach-14 operations. However, due to the modification to control valve operation noted earlier, and the perforations present in the inner liners, the depressurization occurring at the end of a run does not pose a threat.

Figure 15 shows the pressure drop and temperature rise for both the flow restrictor and particle separator under Mach-10 operating conditions. The flow restrictor used for Mach-10 operations is identical in design and material to the one used in Mach-14 operations. The calculations of Appendix C indicate a maximum pressure drop capability of 22,000 psi. In actual Mach-10 testing the restrictor has successfully withstood a 20,000 psi pressure drop at 1500°F.

The particle separator used in Mach-10 operations is similar in principle to the Mach-14 particle separator, but different in size and material. Calculations presented in Appendix C indicate a maximum pressure drop capability of 1700 psi at 1500°F.

CONCLUSIONS

The utilization of the vertical heater vessel for both Mach-14 and Mach-10 testing has been successfully demonstrated. For Mach-14, test Reynolds numbers up to 4.2×10^6/ft are obtainable. For the Mach-10 system, test Reynolds numbers up to 5.6×10^6/ft are a reality. Though this Mach-10 limit was somewhat less than predicted, it is felt that design changes to heater vessel internals and diaphragm area components would ease the constraints on Mach-10 operations that were listed in Table 5, thus allowing for increases in nozzle pressures. (In

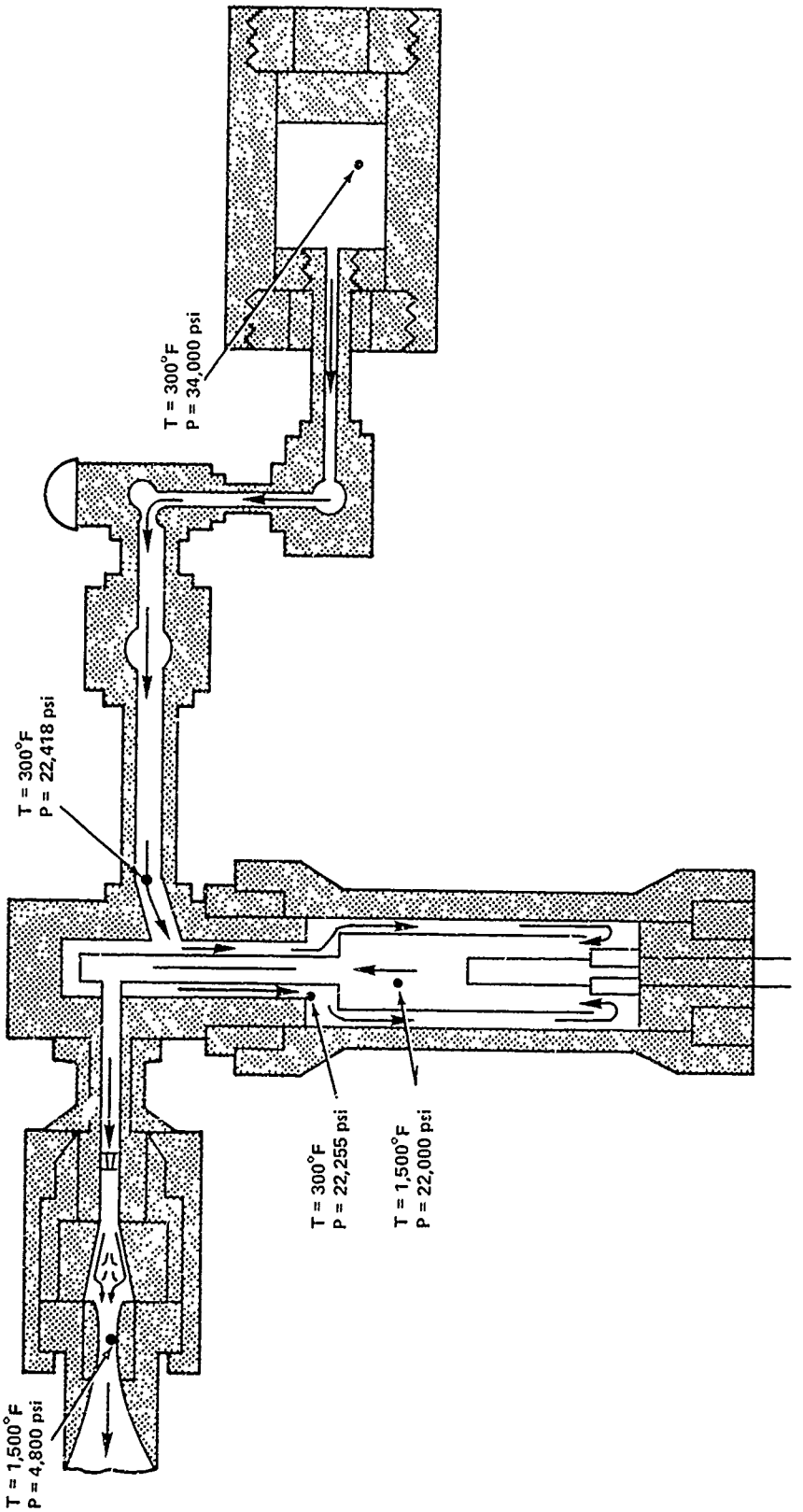

FIGURE 14 GAS CONDITIONS DURING STEADY-STATE FLOW REGIME (MACH-10)

TABLE 6 COMPARISON OF MACH-10 STEADY-STATE PRESSURE DROP WITH STATIC BUCKLING CAPABILITY

COMPONENT	STEADY-STATE PRESSURE DROP	STATIC BUCKLING CAPABILITY
VERTICAL ELBOW OUTER JACKET	418	1400
MAIN HEATER OUTER JACKET	255	1150
HORIZONTAL ELBOW OUTER JACKET	418	600
TOP COVER PLATE	255	690
HEATER SUPPORT RING	255	275

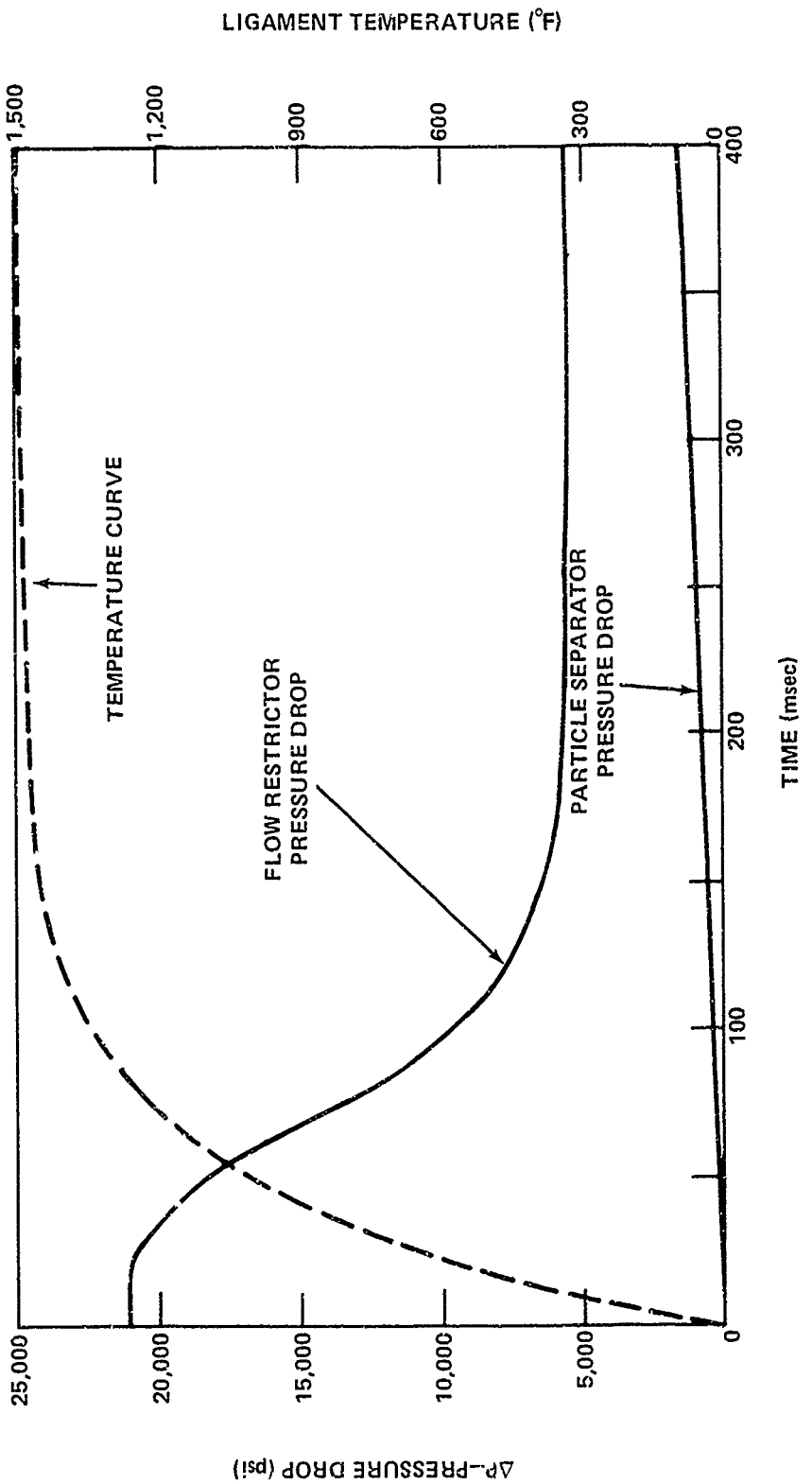

FIGURE 15 PRESSURE DROP(S) & TEMPERATURE RISE VS TIME FOR MACH-10 CONDITION

fact, another program, Mach-10 HIRE (Higher Reynolds number) is presently underway, with a goal of achieving a test Reynolds number of 20 x 10^6/ft, with the vertical heater vessel. Major changes include thicker insulation jackets and liners, a new flow restrictor and a more efficient particle separator.)

For purposes of determining both Mach-14 and Mach-10 operability limits, two portions, or regimes, of a typical tunnel run were investigated; the initial transient condition lasting about 100 msec and the steady-state condition of approximately 800 msec duration during which data is recorded. A principal concern during the transient regime is survivability of heater vessel internals which protect the heater vessel from the hot test gas. These internal components are subjected to a rarefaction wave, resulting from diaphragm burst, which places an oscillating pressure load on the internals. Analyses indicate that for both Mach-10 and Mach-14 operations, ablative flow restrictors are necessary to mitigate this initial transient. Failure of the ablators to function properly could result in buckling of the horizontal and vertical elbow outer jackets, horizontal elbow inner liner, and the heater support ring. Proper functioning of the ablators is critical to successful operational of the tunnel.

During the steady-state regime pressure drops occur due to friction losses in the flow passage from the driver vessels to the throat area. For both Mach-10 and Mach-14 operations analyses indicate these pressures drops do not threaten the structural integrity of the heater internals. The major concerns during the steady-state condition are the pressure drops occurring across a "hot" flow restrictor and particle separator. Analyses and testing have determined the maximum pressure drop capabilities (in the hot condition) to be;

9,240 psi - Mach-14 operation, flow restrictor

320 psi - Mach-14 operation, particle separator

22,000 psi - Mach-10 operation, flow restrictor

1,700 psi - Mach-10 operation, particle separator (inconel)

The depressurization occurring at the end of a run when the control valves close presents no threat to heater internals for Mach-10 or Mach-14 operations.

For purposes of documentation the drawings used for the analyses contained in this report are listed in Table 7. Revision Letters are listed for NSWC drawings only because National Forge and NAVFAC drawings are not revised after acceptance. If a National Forge component requires modification, an NSWC drawing is made of the modified component.

TABLE 7 LIST OF DRAWINGS

DRAWING NUMBER	REV	DRAWING NUMBER	REV	DRAWING NUMBER	REV	NATIONAL FORGE DRAWINGS	NAVFAC DRAWINGS
78E1103	F	75E1534	B	77B1153	–	4-01359	1292571-85
75D1476	–	77C1154	–	77D1155	–	4-01468	1292571-69
75D1477	A	77D1158	A	75F1603	A	2-01309	1292571-73
75[illegible]42	D	77B1229	A	76C1344	A	1-01012	1292531
77D1039	C	77B1228	–	76C1325	A	4-01360	
76D1467	E	77C1085	A	76D1468	E	4-01518	
75E1543	–	77E1089	C	75F1605	B	1-01155	
73B1088	A	78C1106	A	76F1475	–	1-02031	
76D1482	B	77E1090	C	76E1490	A	1-00999	
81D1037	–	77E1203	E	74D2354	B	4-01266	
77C1084	A	77B1081	C	78D1283	A	1-00990	
75D1457	–	77B1079	C	78C1295	–	1-00989	
75D1503	A	78C1104	A	76D1561	–	4-01424	
76C1532	–	77C1088	B	78B1296	–	1-01126	
76D1531	A	77C1159	A	80F1115	–		
76B1535	–	77D1156	–	76E1530	A		
76C1533	A	75D1504	C	78D1304	A		
76C1534	–	73D1439	–	76E1442	B		
77D1157	–	81C1038	–	75D1514	–		
76C1422	A						

BIBLIOGRAPHY

Anderson, D. L. and Lindberg, H. E., "Dynamic Pulse Buckling of Cylindrical Shells Under Transient Lateral Pressures," AIAA Journal, Vol. 6, No. 4, Apr 1968.

Brahinsky, H. S. and Neel, C. A., "Tables of Equilibrium Thermodynamic Properties of Nitrogen," Vol. IV, Aug 1969.

Bruhn, "Analysis and Design of Flight Vehicle Structures," Tri-State Offset Co., 1973 Edition.

Hill, Jacques A. F., "Initial Operation of the NOL Hypervelocity Tunnel," AIAA Paper 74-608, Jul 1974.

Horvay, "The Plane Stress Problem of Perforated Plates," Journal of Applied Mechanics, Vol. 19, 1962.

ODAI Final Report No. 1270-8-79, "Hyper-Velocity Wind Tunnel Components Structural Evaluation," May 1979.

Ragsdale, W. C., "Pershing II Static Stability and Pressure Test in the NSWC Hypervelocity Wind Tunnel," NSWC MP 80-493, Oct 1980.

Roark, R. J., Formulas for Stress and Strain, McGraw-Hill Co., Fourth Edition 1965.

Schneider, A. E., The Physics of Flow Through Porous Media, McMillian Co., New York, 1960.

Streeter, V. L., Fluid Mechanics, McGraw-Hill Book Co., Fifth Edition, 1971.

Timoshenko, Y., Elements of Strength of Materials, Van Nostrand Co., Fifth Edition, 1968.

Timoshenko, Y., Theory of Plates and Shells, McGraw-Hill Book Co., Second Edition 1968.

TERMS

a - Sound Speed (ft/sec)

A - Area (ft^2)

K_n - Nozzle Discharge Coefficient

p - Pressure

u - Gas Velocity (Ft/sec)

γ - Isentropic Exponent $(dp/D\rho)s$

ρ - Gas Density (lb/ft^3)

Δp - Pressure Drop (lb/in^2)

Subscript

H - Heater Region

R - Restrictor Region

Superscript

* - Sonic Throat Region

APPENDIX A

BUCKLING PRESSURE CAPABILITIES OF MACH-14 HEATER INTERNALS

Buckling strength capabilities for the insulation package components were computed for both static and dynamic loading conditions. The static buckling pressures were obtained via a method contained in Reference A-1. The dynamic buckling pressures were obtained via a method contained in Reference A-2.

Values of Young's modulus in the tables below were degraded due to temperature effects. In the case of the inner liners, the values of "E" were further degraded (usually by 10%) to account for the weakening effect of the vent holes.

STATIC BUCKLING PRESSURES-P_{CR}

The principal buckling equation used for static buckling, is

$$P_{CR} = \frac{k_p \pi^2 E}{12(1-\nu^2)} \frac{t}{R} \left(\frac{t}{L}\right)^2 \qquad \text{(A-1)}$$

where k_p - (obtained from Reference A-1) geometric property of the cylinder in question,
t - cylinder thickness (in)
R - cylinder radius (in)
L - cylinder length (in)
ν - Poisson's ratio for cylinder material

The table below contains values of these parameters for the various liners, and the value of P_{CR} obtained. To ensure the values of P_{CR} are in the elastic range of the material, a buckling pressure - P_E, corresponding to the yield strength of the material was calculated using;

A-1 Bruhn, "Analysis and Design of Flight Vehicle Structures," Tri-State Offset Co., 1973 Edition.

A-2 Anderson, D. L. and Lindberg, H. E., "Dynamic Pulse Buckling of Cylindrical Shells Under Transient Lateral Pressures," AIAA Journal, Vol. 6, No. 4, Apr 1968.

$$P_E = \frac{\sigma_Y t}{R} \qquad \text{(A-2)}$$

where σ_Y = yield strength of the cylinder material (psi)

As can be seen from the values listed, all buckling pressure values - P_{CR}, are below their cylinder's respective P_E.

Component	t(in)	R(in)	L(in)	K_p	ν	E(psi)	σ_Y(Psi)	P_{CR}(psi)	P_E(psi)
Vertical Elbow Outer Jacket	.25	4.25	73	80	.3	28×10^6	40,000	1400	2350
Main Heater Outer Jacket	.5	11.5	106	47	.3	28×10^6	40,000	1150	1740
Horizontal Elbow Outer Jacket	.1	2.95	43	110	.3	22×10^6	30,000	400 *(600)	1020
Vertical Elbow Liner	.1	2.8	80	NA	.3	12×10^6	30,000	*150	1070
Main Upper Heater	.5	9.75	55	25	.1	1.35×10^6	7,000	120	360
Liner Lower	.5	10.1	42.5	21	.1	1.35×10^6	7,000	160	350
Horizontal Elbow Liner	.125	2.06	46	1[illegible]	.3	15×10^6	30,000	910	1820

The two values of P_{CR} marked by an asterisk were obtained by methods different than the one described previously. Equation (A-1) was not applicable to the vertical elbow liner's geometry. Instead, the following buckling equation was employed:[A-3]

$$P_{CR} = \frac{E}{4(1-\nu^2)} \left(\frac{t}{R}\right)^3 \qquad \text{(A-3)}$$

Use of this equation results in a P_{CR} for the vertical liner as shown in the table above.

The value of 400 psi for the horizontal elbow outer jacket was obtained by use of Equation (A-1). However, this liner has a .050 in thick liner wrapped around the circumference. To account for the benefit of increased thickness, the following analysis was used.

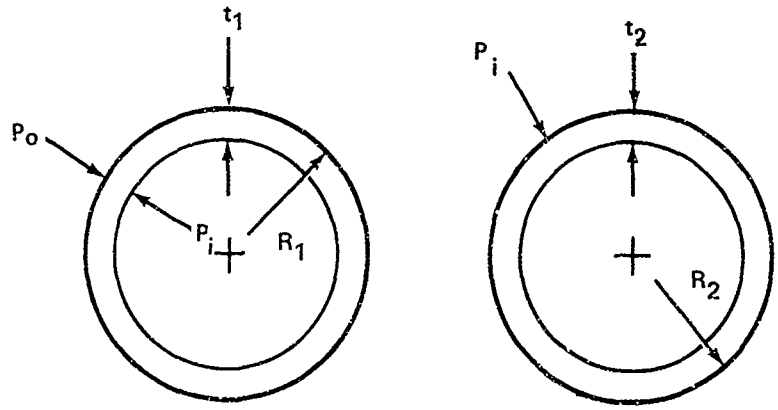

It is assumed that a pressure P_i is applied to the inner cylinder. It is desired to find what P_o must be applied to the outer cylinder to give this P_i on the inner cylinder. This is done by equating the deflections of the two cylinders. In equation form;

Deflection of outer cylinder $\delta_o = (P_o - P_i) \left(\frac{R_1^2}{E_1 t_1}\right)\left(1 - \frac{\nu_1}{2}\right)$

[A-3] Roark, R. J., Formulas for Stress and Strain, McGraw-Hill Co., Fourth Edition, 1965.

Deflection of inner cylinder $\delta_i = P_i\left(\frac{R_2^2}{E_2 t_2}\right)\left(1 - \frac{\nu_2}{2}\right)$

For a similar material, $E_1 = E_2$, $\nu_1 = \nu_2$.

Equating δ_o with δ_i and eliminating like terms yields;

$$(P_o - P_i)\ \frac{R_1^2}{t_1} = P_i\ \frac{R_2^2}{t_2} \qquad \text{(A-4)}$$

using $R_1 = 3"$ $\quad R_2 = 2.95"$
$t_1 = .05"$ $\quad t_2 = .1"$

and $P_i = 400$ psi

in Equation (A-4) results in a P_o of 600 psi. Thus, to reach a P_{CR} of 400 psi on the inner cylinder requires an external pressure of 600 psi on the outer cylinder. The combination of the inner cylinder wrapped with a .050 inch thick liner thus has a buckling pressure capability of 600 psi.

The dynamic buckling pressure P_D, of each cylinder was computed using a method described in Reference A-2.

If the pressure is highly impulsive there will be an enhancement in the critical buckling pressure. The buckling or damage curve is illustrated below:

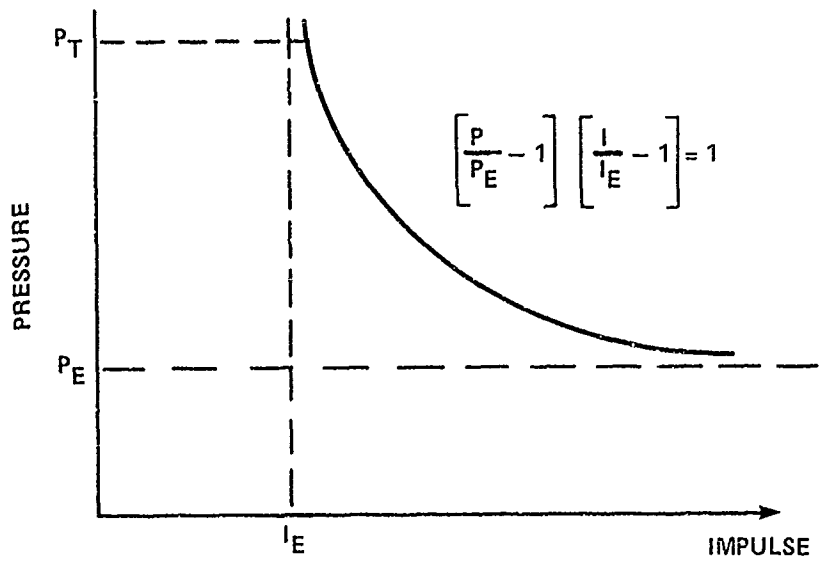

A-2 See footnote A-2 on page A-1.

If the time duration (hence impulse) is large compared to the natural period, the shell buckles in a quasistatic manner at P_E where P_E is the elastic static buckling pressure (previously computed). If the loading is impulsive, the buckling presure increases asymptotically to the elastic impulse line:

$$I_e = \frac{5\rho c}{g} R\,(t/R)^2$$

where ρ = density of cylinder material

$$c = \text{sound speed} = \left(\frac{E}{\rho}\, g\right)^{1/2}$$

The region between the Asymptotes is defined by Hyperbola

$$\frac{P}{P_E} - 1 \quad \frac{I}{I_E} - 1 \quad = 1$$

Assuming a triangular pulse is applied, which approximates the spikes observed in the pressure traces obtained in the Mach-14 cold shake down tests, then

$$I = \frac{1}{2} \quad P_{max}\ T_{max}$$

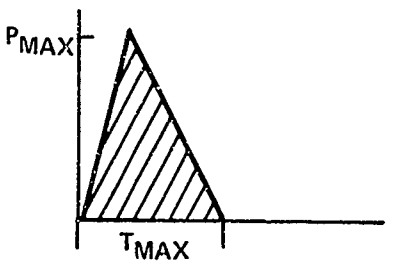

To find the dynamic buckling pressure "P_D",

$$P_D = P_{max}$$

Thus,

$$\left[\frac{P_D}{P_E} - 1\right] \left[\frac{1}{2} \quad \frac{P_D\ T_{max}}{I_E} - 1\right] = 1$$

Solving Yields:

$$P_D = P_E + \frac{2\ I_E}{T_{max}} \qquad \text{(A-5)}$$

The table below contains values of ρ, c, I_e, T_{max}, P_{CR} and lastlv P_D for the cylinders of interest. Note the increase in buckling capability when the load is applied in an impulsive manner.

Component	Density (lb/in^3)	C-Sound Speed (in/sec)	IE-Elastic Impulse (psi-sec)	T_{max} (psi)	P_E (psi)	P_D (psi)
Vertical Elbow Outer Jacket	.29	193,000	10.5	10.5	2350	4350
Main heater Outer Jacket	.29	193,000	15.7	3.0	1740	12,200
Horizontal Elbow Outer Jacket	.29	171,000	2.2	10.5	1020	1440
Vertical Elbow Inner Liner	.37	112,000	1.9	10.5	1070	1430
Main heater Upper Liner	.064	90,000	1.9	3.0	360	1620
Lower Liner	.064	90,000	1.8	3.0	350	1550
Horizontal Elbow Inner Liner	.37	125,000	4.5	10.5	1820	2680

Two additional heater internal components required analysis to determine their ability to survive the rarefaction wave.

As the wave passes through the main heater section, an external pressure load is applied to the top cover plate of the main heater insulation package as shown below. This load is also transmitted to the heater support ring at the bottom of the heater. Both of these components will now be analyzed to determine their buckling load capabilities.

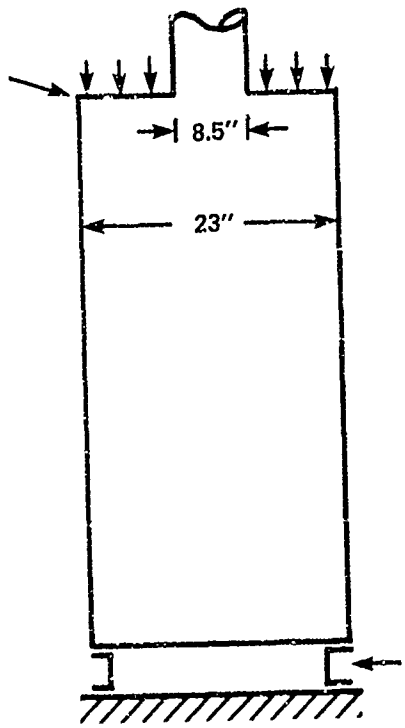

TOP COVER PLATE

The top cover plate is fabricated from carbon steel having yield strength of 40,000 psi.

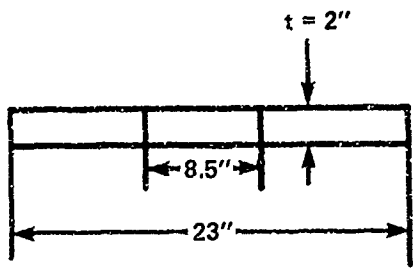

To determine the cover plate's buckling pressure capability, the loading condition on the plate is approximated by the condition shown below:

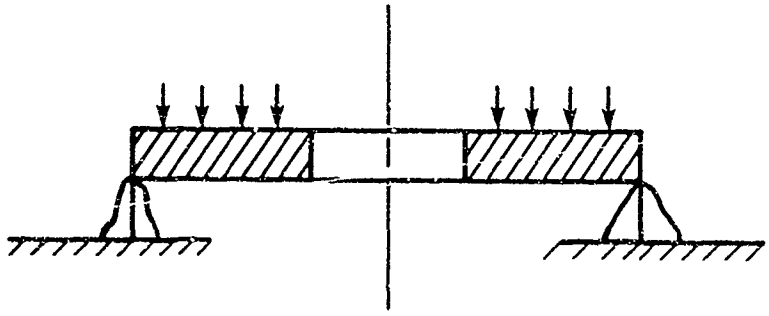

The plate is assumed to be simply supported on the outer edge and free on the inner edge. This loading condition is analyzed in Reference A-4. The following Equation, obtained from Reference A-4 is used to determine the cover plate's P_{CR}:

$$P_{CR} = \frac{\sigma_Y t^2}{k\ a^2} \qquad \text{(A-6)}$$

where σ_Y = yield strength of the material
= 40,000 psi

t = plate thickness = 2"

k = factor based on ratio of plate O.D. to plate I.D.
(for $\frac{O.D.}{I.D.} = \frac{23}{8.5} = 2.7$) k = 1.75

a = outer radius = 11.5 in

Substitution Yields

$$P_{CR} = \frac{40{,}000\ (2)^2}{1.75\ (11.5)^2} = 690 \text{ psi}$$

The top cover plate thus has a static buckling capability of 690 psi.

A-4 Timoshenko, Y., Theory of Plates and Shells, McGraw-Hill Book Co., Second Edition, 1968.

HEATER SUPPORT RING

The heater support ring bolts to the closure plug and supports the main heater's inner liner and outer jacket as shown. The ring is strengthened by gussets, .312" thick, on either side of the eight bolt hole locations. Any pressure acting on the top cover plate is transferred, via the outer insulation jacket, to the gussets. To determine the load capability of the gussets, they will be treated as short struts, eccentrically loaded, as shown. The load required to yield a gusset is obtained by using the following equation:[A-5]

$$F = \frac{\sigma_Y}{\frac{1}{A} + \frac{eY}{I}} \qquad \text{(A-7)}$$

where σ_Y = yield strength of material
= 40,000 psi
A = surface area of loaded surface
= (.312) (1.625) = .507 in^2
e = distance from neutral axis to load application point
= .6125 in
Y = distance from neutral axis to remote fiber crossection
= .8125 in
I = moment of inertia of loaded surface cross section
= $\frac{1}{12}$ (.312) $(1.625)^3$ = .11 in^4

Substitution into Equation (A-7) yields:

$$F = \frac{40{,}000}{\left[\frac{1}{.507} + \frac{.6125(.8125)}{.11}\right]}$$

F = 6157 lbs

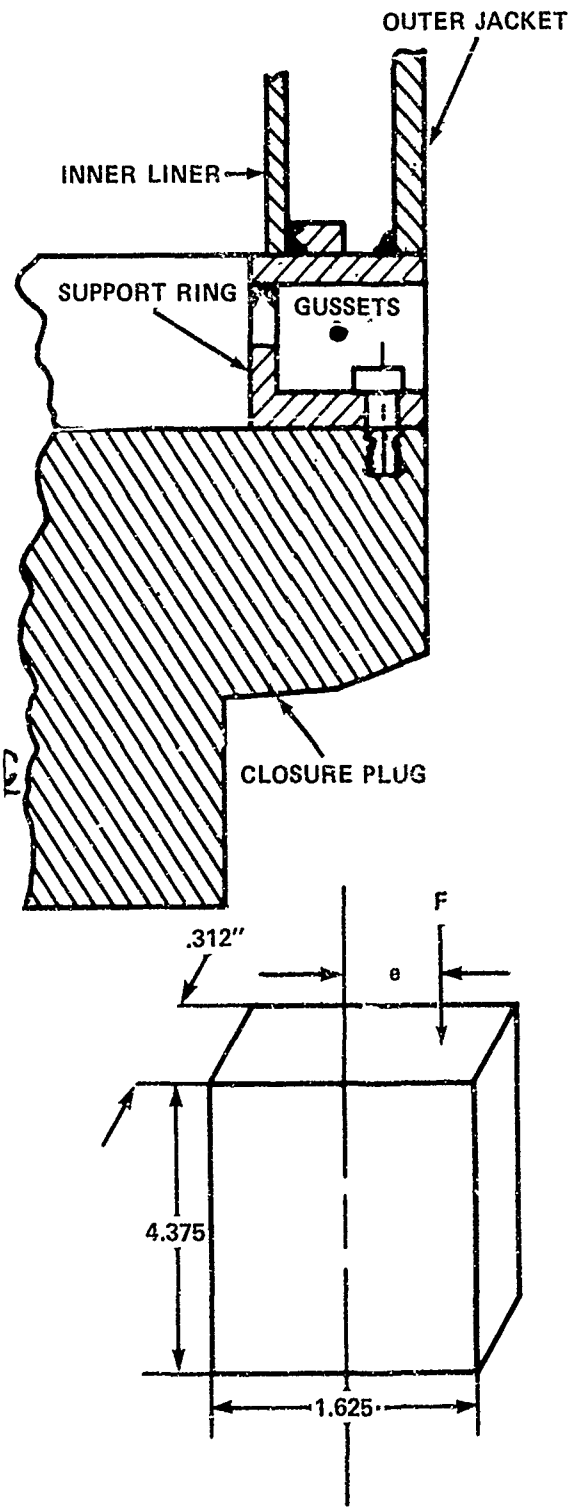

[A-5] Timoshenko, Y., Elements of Strength of Materials, Van Nostrand Co., Fifth Edition, 1968.

Thus the total load the ring can take is

$$F_T = 16 \times F = 16 \times 6137 = 98{,}512 \text{ lbs}$$

This must now be converted to a pressure acting on the top cover plate. Recall

$$p \cdot A_L = F_T$$

where A_L cover plate area $= \frac{\pi}{4} (23^2 - 8.5^2) = 359 \text{ in}^2$,

$$F_T = 98{,}512 \text{ lbs}$$

Substitution yields:

$$p = \frac{98{,}512}{359}$$

$$P = 275 \text{ psi}$$

Thus the heater support ring will withstand a pressure of 275 psi acting across the top cover plate.

APPENDIX B

POROSITY EFFECT ON INNER LINER PRESSURE DROP

As noted in the main report, the initial reason the inner liners were perforated was to prevent the rapid depressurization occurring at the end of a run from collapsing the liners. However, venting the liners also serves to alleviate the effect of the depressurization which occurs as a result of the rarefaction wave passing over the liners.

A normalized rate of change of pressure in various sections of the heater can be estimated from;

$$\frac{1}{P_H}\frac{dp}{dt} \qquad \text{(B-1)}$$

where P_H = heater pressure
dp = initial pressure drop (shown in Figure 3 in the main text)
dt = time of the initial pressure drop

Values of dp for various sections of the heater are obtained from Figures 4, 5, and 6 in the main text. However, the values obtained from these figures must be halved due to the fact they are peak to peak valves.

To estimate the effect perforating a liner will have on the pressure drop experienced by the liner, J. Hill, in a series of NSWC memos, concluded the pressure drop across a porous shell was equivalent to the dynamic head pressure of the gas moving through a vent hole.

In equation form;

$$\Delta p = \frac{1}{2}\rho V_h^2$$

where ρ = density of gas in insulation volume (slugs/ft^3)
V_h = velocity of gas moving through a vent hole (ft/sec)

The velocity of gas moving through porous insulation is given as;[B-1]

$$V = .9 \frac{Vi}{A} \frac{1}{\gamma} \frac{1}{P_H} \frac{dp}{dt} \tag{B-3}$$

where Vi = insulation volume (ft^3)
A = liner surface area (ft^2)
γ = isentropic exponent

For a perforated liner, the velocity at the hole is determined from

$$V_h = \frac{V}{PC_D} \tag{B-4}$$

where P = porosity
C_D = dishcarge coefficient = .6

Substitution of V from Equation (B-3) in Equation (B-4) yields

$$V_h = .9 \frac{Vi}{A} \frac{1}{\gamma} \frac{1}{P_H} \frac{dp}{dt} \frac{1}{PC_D} \tag{B-5}$$

Now substituting for V_h in Equation (B-2) yields,

$$\Delta p = \frac{1}{2} \rho \left[.9 \frac{Vi}{A} \frac{1}{\gamma} \frac{1}{P_H} \frac{dp}{dt} \left(\frac{1}{PC_D} \right) \right]^2 \left(\frac{1}{144} \right)^2 \tag{B-6}$$

The ratio of Vi/A is simply the insulation thickness. Thus having values of $1/P_H$ dp/dt, the pressure drop across a given liner can be determined.

MACH-14 OPERATION

For a P_H = 22,000 psi, the following are values of $1/P_H$ dp/dt for different sections of the heater, under normal and abnormal ablator function conditions.

[B-1] Schneider, A. E., The Physics of Flow Through Porous Media, McMillian Co., New York, 1960.

TABLE B-1 DEPRESSURIZATION RATES (MACH-14)

Heater Section	(dp) Normal Ablation (psi)	(dp) Ablator Failure (psi)	dt (msec)	$\left(\frac{1}{P_H}\frac{dp}{dt}\right)$ Normal Ablation	$\left(\frac{1}{P_H}\frac{dp}{dt}\right)$ Ablator Failure
Horizontal Elbow	220	1615	1.5	6.7	49
Vertical Elbow	110	800	1.5	3.3	24
Main Heater	15	105	1.5	.5	3

For nitrogen at 22,000 psi and approximately 1500°F (in the insulation), γ and ρ are obtained from Reference B-2,

$$\gamma = 2$$

$$\rho = 19.5 \frac{lb}{ft^3} = .61 \frac{slugs}{ft^3}$$

Using these values, along with the values of $1/P_H$ dp/dt listed above in Table B-1 and the insulation thicknesses and porosities shown below in Table B-2, in Equation (B-6), results in determination of Δp across various liners.

B-2 Brahinsky, H. S. and Neel, C. A., "Tables of Equilibrium Thermodynamic Properties of Nitrogen," Vol. IV, Aug 1969.

TABLE B-2 PRESSURE DROPS ACROSS VENTED LINERS (MACH-14)

Heater Section	$\frac{Vi}{A}$ (ft)	p-porosity	(Δp) Normal Ablation (psi)	(Δp) Ablator Failure (psi)
Horizontal Elbow	.065	.005	9	483
Vertical Elbow	.106	.012	1	53
Main Heater Upper	.104	.012	.023	.81
Main Heater Lower	.075	.012	.012	.41

Comparing the values (Δp) listed in Table B-2 for a vented liner, with the values (dp) shown in Table B-1 for an unvented liner it can be seen the pressure drop across each liner is reduced by a order of magnitude in every case except the horizontal elbow under ablator failure conditions.

MACH-10 OPERATION

In Mach-10 operation the normalized rates of change computed will be slightly different due to the lower gas temperatures involved. The values of dp shown in Table B-1 are applicable to the Mach-10 case. However, as shown in Appendix E, the time of the initial pressure drop is somewhat longer, 1.65 milliseconds. Table B-3 below contains values of $1/P_H$ dp/dt for various sections of the heater.

TABLE B-3 DEPRESSURIZATION RATES (MACH-10)

Heater Section	dp (psi) (Normal)	dp (psi) (Abnormal)	dt (msec)	$\left(\frac{1}{P_H}\frac{dp}{dt}\right)$ (Normal)	$\left(\frac{1}{P_H}\frac{dp}{dt}\right)$ (Abnormal)
rizontal Elbow	220	1615	1.65	6	44
Vertical Elbow	110	800	1.65	3	22
Main Heater	15	105	1.65	.4	3

For a P_H of 22,000 psi and a gas temperature in the insulation of 700°F,

$$\gamma = 2.8$$

$$\rho = 27 \frac{lb}{ft^3} = .84 \frac{slugs}{ft^3}$$

Using the above values in Equation (B-6) with the porosities and insulation thickness given in Table B-4, results in the pressure drops given in Table B-4 below.

TABLE B-4 PRESSURE DROPS ACROSS VENTED LINERS (MACH-10)

Heater Section	$\frac{Vi}{A}$ (ft)	p porosity	(Δp) Normal Ablation (psi)	(Δp) Ablator Failure (psi)
Horizontal Elbow	.065	.005	5.1	274
Vertical Elbow	.106	.012	.6	32
Main	.104	.012	.01	.57
Upper Heater Lower	.075	.012	.005	.29

As in Mach-14 operation, the pressure drop (Δp) across a vented liner is much less than the pressure drop (dp) across an unvented liner.

The venting of the liners has the additional benefit of allowing use of a thinner liner, thus occupying less internal volume of hot test gas.

APPENDIX C

FLOW RESTRICTOR AND PARTICLE SEPARATOR ANALYSES

FLOW RESTRICTOR

As noted earlier, the flow restrictor used for both Mach-14 and Mach-10 operations in the Mach-14 Heater vessel is identical in geometry and material. A finite element heat transfer analysis indicated, for both Mach-14 and Mach-10 operations:

1. The inner wall temperature of the seven restrictor holes rises to 90% of the free stream gas temperature very rapidly (<200 msec),

2. The average temperature of the "ligaments" between holes rises to 60% of the free stream gas temperature rapidly (<500 msec).

Due to the conclusions noted above, the material (Columbium C-103) used in the flow restrictor design must have excellent high temperature properties. Figure C-1 is a graph of Columbium's yield strength vs temperature.

Past analyses of the flow restrictor usually encompassed two loading conditions; the first being the full heater pressure (22,000 psi) acting over a "cold" flow restrictor at the beginning of a run, and the second being some maximum Δp acting across a "hot" restrictor later in the run. The cold condition for Mach-14 and Mach-10 operation is the same due to the same maximum heater pressure used. However, the hot conditions vary from Mach-14 to Mach-10 due to the different gas temperatures involved.

The flow restrictor can be treated as a thick plate, thus shear stresses occurring in the plate are of first order importance. In fact, a previous design of the flow restrictor did fail in shear at the shoulder support location (see Figure 7 in the main report). The two areas where shear stresses will be evaluated are at the 3.25 inch diameter already noted, and at the 2.2 inch hole diameter where the restrictor plate is weakened due to the presence of holes through the plate.

COLD CONDITION

$$\Delta p = 22{,}000 \text{ psi}$$

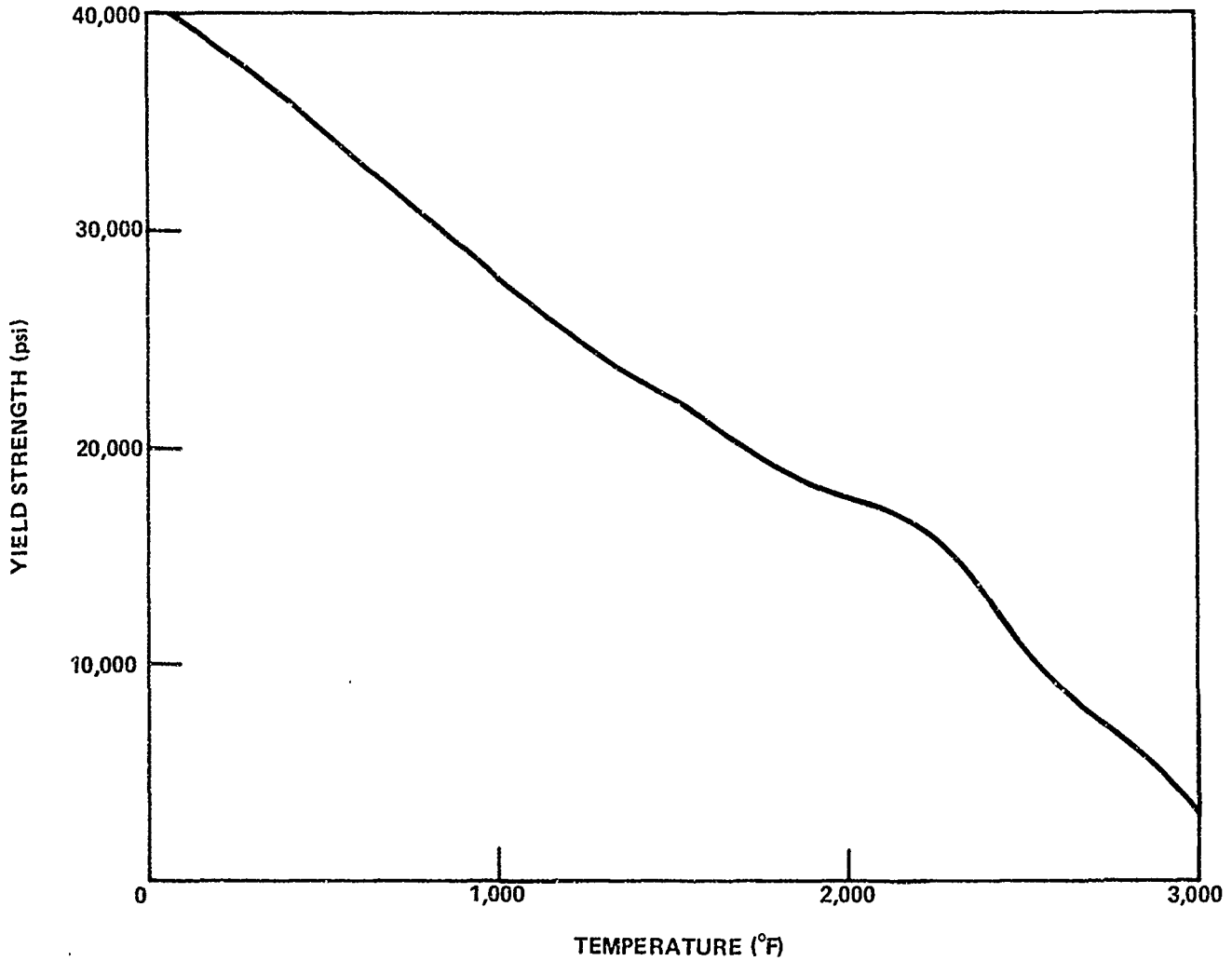

FIGURE C-1 COLUMBIUM'S YIELD STRENGTH VS TEMPERATURE CURVE

The shear stress in the plate is calculated from

$$\tau = \frac{\Delta p\ (A_L)}{A_S} \qquad \text{(C-1)}$$

where A_L is the loaded area of the plate (in^2)
A_S is the shear area (in^2)

First examine the shear stress at the 3.25 inch diameter section. At this section,

$$A_L = \begin{pmatrix} \text{area of plate} \\ \text{out to 3.25" dia} \end{pmatrix} - \begin{pmatrix} \text{area of 7 holes} \end{pmatrix}$$

$$A_L = \pi \left(\frac{3.25^2}{4}\right) - 7 \cdot \left(\frac{\pi}{4} \cdot 46^2\right)$$

$$A_L = 7.13\ in^2$$

and A_S = (circumference at 3.25 in. dia) x (plate thickness) = πdt where t is the plate thickness. Thus,

$$A_S = \pi(3.25)(1.75)$$

$$A_S = 17.87\ in^2$$

Substitution into Equation (C-1) yields

$$\tau = \frac{22{,}000\ (7.13)}{(17.87)}$$

$$= 8780\ psi$$

Next calculate the shear stress at the 2.2 inch hole diameter. For this section,

$$A_L = \begin{pmatrix} \text{area of plate} \\ \text{out to 2.2" dia} \end{pmatrix} - \begin{pmatrix} \text{area of 4 holes} \end{pmatrix}$$

(Note 4 holes are comprised of 6 half-holes and 1 complete hole)

Thus,

$$A_L = \left(\frac{\pi}{4} \cdot 2.2\right) - 4 \cdot \frac{\pi}{4} \cdot 46^2$$

$$A_L = 3.14\ in^2$$

Next calculate A_S:

$$\left[A_S = \pi d - 6(\text{hole diameters})\right] (\text{plate thickness})$$

$$A_S = \left[\pi(2.2) - 6(.46)\right] (1.75)$$

$$A_S = 7.27 \text{ in}^2$$

Substitution into Equation (C-1) yields:

$$\tau = \frac{22{,}000\ (3.14)}{7.27}$$

$$\tau = 9500 \text{ psi}$$

Based on Tresca shear stress failure criteria, the allowable shear is 57% of the yield strength of the material. Referring to Figure C-1, the yield strength of columbium at 100°F is 40,000 psi. Thus the allowable shear stress is .57 x 40,000 psi or 22,800 psi. The shear stresses calculated above are much lower than the allowable value, thus the flow restrictor will not fail in shear under the full heater pressure in the cold condition. This applies to both Mach-14 and Mach-10 operations.

HOT CONDITION

Due to the reduction in material yield strength at elevated temperatures it is not certain as to whether the flow restrictor could withstand the full heater pressure in the hot condition. Thus, for the hot condition, Equation (C-1) will be employed, but this time an acceptable Δp will be determined based on an allowable shear stress. For the hot condition the Mach-14 case and Mach-10 case must be treated separately.

1. MACH-10 CASE. As noted earlier, in the hot condition the restrictor hole's wall temperature is 90% of the free stream gas temperature. In the Mach-10 case, the wall temperature is thus .9 x 1500 or 1350°F. Referring to Figure C-1, at a temperature of 1350°F Columbium has a yield strength of 21,500 psi. Thus the allowable shear stress at this temperature is .57 x 21,500 psi or 12,255 psi. Recalling the shear stress values obtained for a Δp of 22,000 psi (8780 psi at the 3.25 inch dia, 9500 psi at the 2.2 inch hole dia), it can be seen that the flow restrictor can in fact withstand the full heater pressure in the hot (Mach-10) condition.

2. MACH-14 CASE. The free stream gas temperature in the Mach-14 case is 3000°F. Thus the flow restrictor hole's wall temperature is .9 x 3000°F or 2700°F. The average ligament temperature is .6 x 3000°F or 1800°F. In order to have some margin on material property uncertainties, the allowable shear stress that will be used in calculating an allowable pressure load will be obtained by using the yield strength properties of Columbium at 2700°F. Referring again to Figure C-1, at 2700°F Columbium's yield strength is 7000 psi. This translates into an allowable shear stress of .57 x 7000 psi or 3990 psi.

At the 3.25 inch dia, the Δp for an allowable shear stress of 3990 psi is, from Equation (C-1);

$$\Delta p = \frac{\tau \cdot A_S}{A_L}$$

Substitution yields;

$$\Delta p = \frac{3990\ (17.87)}{(7.13)}$$

$$\Delta p = 10{,}000 \text{ psi}$$

Similarly at the 2.2 inch hole diameter,

$$\Delta p = \frac{\tau A_S}{A_L}$$

Thus,

$$\Delta p = \frac{3990\ (7.27)}{(3.14)}$$

$$\Delta p = 9240 \text{ psi}$$

Thus the maximum allowable Δp is the lesser of the two values obtained above, or 9240 psi.

The table below contains a summary of the results obtained for both Mach-10 and Mach-14 loading conditions using the 7-hole Columbium flow restrictor.

PRESSURE DROP CAPABILITIES OF COLUMBIUM FLOW RESTRICTOR

	COLD CONDITION	HOT CONDITION
MACH-14	22,000 psi	9240 psi
MACH-10	22,000 psi	22,000 psi

It must be remembered the values obtained above were based on shear stress allowables. Bendings stresses have been considered a secondary effect due to the thickness of the plate. In actual wind tunnel testing conducted thus far the flow restrictor has been exposed to a maximum pressure drop of 20,000 psi in Mach-10 operation, and a maximum pressure drop of 2000 psi in Mach-14 use. The larger the pressure drop range, the larger the Reynolds number range testing capability. This is because the test Reynolds number is proportional to P_o, which is a function of pressure drop across the flow restrictor. Thus it appears that lower Reynolds numbers could be obtained in Mach-14 operation by increasing the pressure drop across the flow restrictor from 2,000 psi to some larger value.

PARTICLE SEPARATOR

The particle separators used in Mach-10 and Mach-14 operations are similar in function but different in size and material due to the gas temperatures and mass flow rates involved. The separators are used to remove particles from the gas flow that could damage test models located downstream. The principle of separation is one in which the inertia of the particle is used to remove the particle from the gas stream by turning the flow through the separator without turning the particle. The separators (shown in Figures C-2 and C-3) are subjected to both a pressure drop and an axial force on the nose.

The axial force on the nose arises due to the dynamic head pressure of the nitrogen gas impinging on the front of the particle separator. The pressure drop occurs due to changes in gas flow direction and changes in flow area as the gas proceeds through the particle separator region.

In the following analysis the separators are assumed to be at the gas temperature after a very short time. Bearing stresses are computed to ensure yielding will not occur and a buckling capability of the separators is determined.

MACH-10 SEPARATOR

The Mach-10 separator (Figure C-2) is fabricated from Inconel X-750 which has a yield strength of 40,000 psi at 1500°F. The geometry of the housing around the separator, and the hole sizes and location were chosen to optimize particle separation effectiveness.

The dynamic head pressure of the gas impinging on the nose of the separator must first be determined. In normal operations, the gas impinging on the nose of the separator is at 6000 psi and 1500°F. The density of nitrogen under these conditions is 7.3 lb/ft^3. The maximum mass flow rate is 270 lb/sec. The velocity of the gas impinging on the nose of the separator is determined from:

$$V = \frac{\dot{m}}{\rho A} \qquad (C\text{-}2)$$

where $\dot{m}$ = 270 lb/sec
ρ = 7.3 lb/sec^3
A = flow passage area just upstream of the separator
= 2" x 2" = 4 in^2 = .028 ft^2

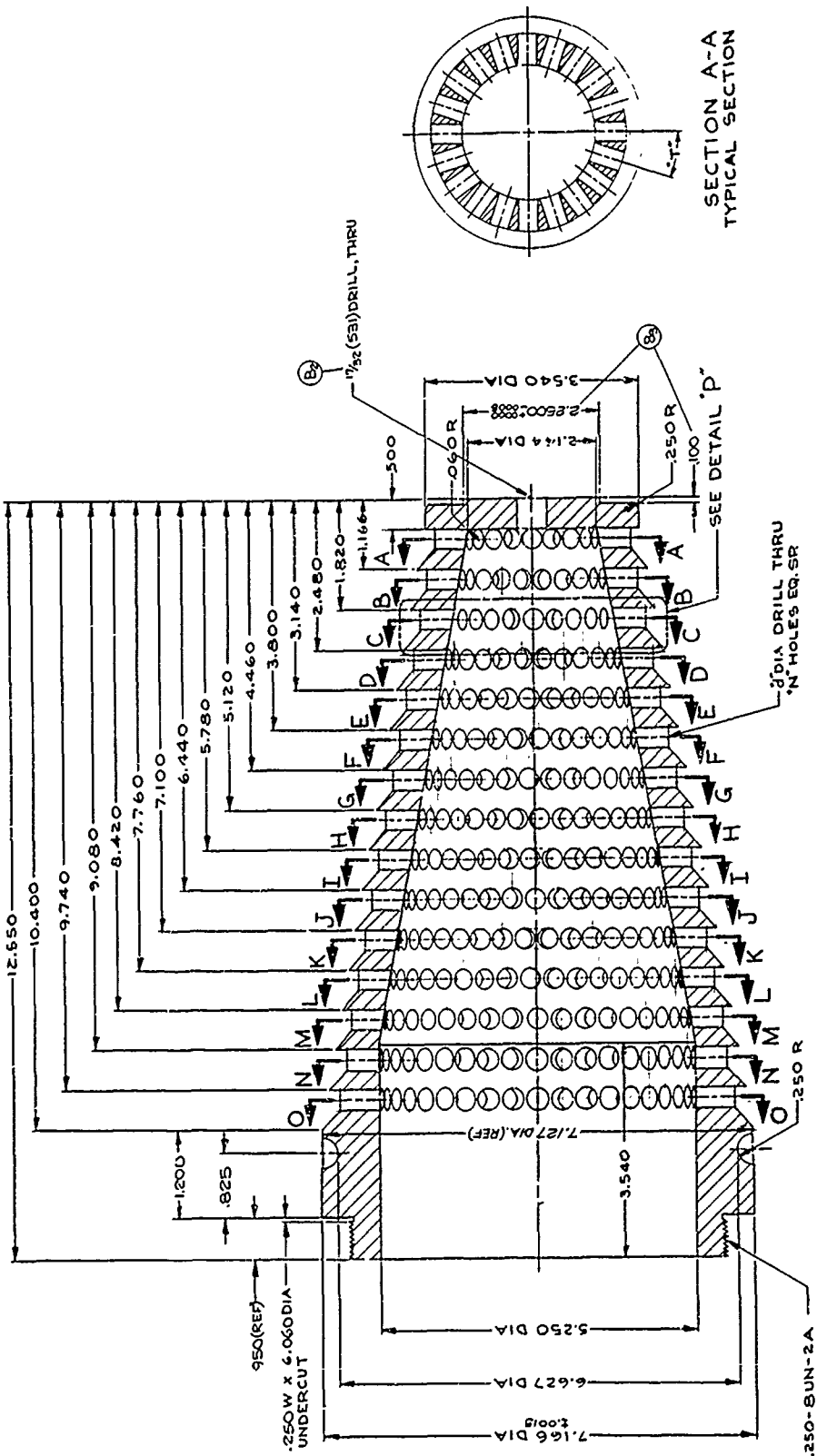

FIGURE C-2 MACH-10 PARTICLE SEPARATOR

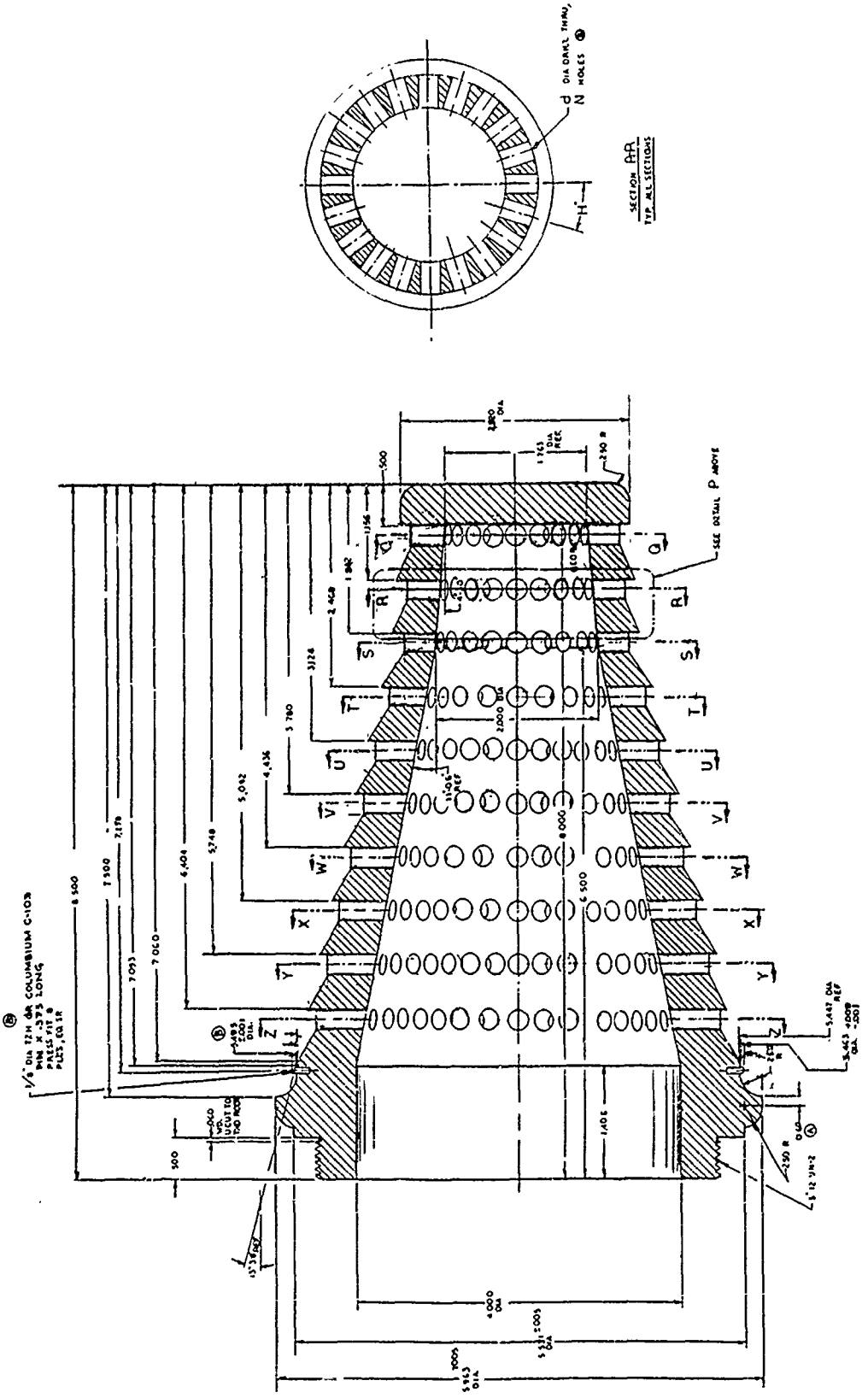

FIGURE C-3 MACH-14 PARTICLE SEPARATOR

Solving for velocity in Equation (C-2) yields:

$$V = \frac{270}{7.3\ (.028)}$$

$$V = 1320 \text{ ft/sec}$$

The dynamic head pressure "q" is determined from:

$$q = \frac{1}{2} \rho V^2 \qquad \text{(C-3)}$$

Thus

$$q = \frac{1}{2} \frac{7.3}{32.2} \left(1320\right)^2$$

$$q = 197{,}500 \text{ lb/ft}^2 = 1370 \text{ lb/in}^2$$

The bearing stresses in the separator will be a maximum where the crossectional area is a minimum. These areas are where the radial holes are located. The total bearing load on any crossection has two components, the first arising from the dynamic head pressure acting on the nose of the separator, and the second being the pressure difference acting on an exposed surface.

Three crossections will be analyzed for the above described condition sections A, H, and O as shown in Figure C-2. The bearing load due to the dynamic head pressure acting on the particle separator is constant for all crossections and is determined from:

$$F_1 = qA \qquad \text{(C-4)}$$

where $q = 1370$ psi
$A = 2 \times 2 = 4 \text{ in}^2$

Thus

$$F_1 = 1370\ (4) = 5480 \text{ lbs.}$$

The force due to a pressure drop through the separator is dependent on the exposed area over which it acts. For instance, the bearing load at crossection "O" due to the pressure drop across the restrictor is based on the net exposed area just upstream of "O" as shown in Figure C-2.

The maximum allowable Δp across the particle separator can be computed from the following equation for bearing stress σ_B,

$$\sigma_B = \frac{F_1 + F_2}{A} \qquad \text{(C-5)}$$

where F_1 = 5,480 lbs due to dynamic pressure
$F_2 = \Delta p\ A_E$ (A_E = exposed area)
A = crossectional area

Substituting into (C-3) and rearranging yields:

$$\Delta p_{max} = \frac{\left(\sigma_B \cdot A\right) - F_1}{A_E}$$

Recall that Inconel X-750 at 1500°F has a yield strength of 40,000 psi. If σ_B is set equal to this value, Δp_{max} for the three crossections of interest may be obtained.

The table below contains values of Δp_{max} for the three crossections of interest. Section A gives the lowest value of Δp_{max}. Thus, the largest pressure drop allowed across the particle separator is 1700 psi.

Crossection	A-Crossection Area (in^2)	A_E-Net Exposed Area (in^2)	Δp_{max} (psi)
A	.606	9.842	1900
H	1.070	21.648	1700
O	2.314	37.360	2330

An estimate of the external pressure required to buckle the particle separator will now be made. Due to the particle separator's geometry, the three crossections analyzed earlier will be treated as rings subjected to an external pressure. The critical buckling pressure of a ring, P_{CR}, is determined from:

$$P_{CR} = \frac{E}{4(1-\nu^2)} \left(\frac{t}{R}\right)^3 \qquad \text{(C-6)}$$

where E = Young's modulus (psi)
ν = poisson's ratio = .3
t = thickness of ring (in)
R = mean radius (in)

To take into account the weakening effect of the holes the values of Young's modulus and Poisson's ratio to be used in Equation (C-6) were changed using a method outlined in Reference C-1. The method used is based on the relative hole spacing and the size of the holes involved. The end result is that an E* and ν^* are computed and used in Equation (C-6) in lieu of E and ν. For the Mach-10 particle separator,

$$E^* = .2\ E$$
$$\nu^* = 1.6\nu$$

For Inconel X-750 at 1500°F, $E = 24 \times 10^6$ psi and $\nu = .3$. Thus,

$$E^* = .2\ (24 \times 10^6) = 4.8 \times 10^6 \text{ psi}$$

$$\nu^* = 1.6(.3) = .48$$

Using the values shown above in conjunction with the thicknesses and mean radii given in the table below, values of P_{CR} were obtained for the three crossections of interest.

Crossection	t (in)	R (in)	P_{CR} (psi)
A	.37	1.5	23,4000
H	.40	2.37	7,500
O	.54	3.17	7,700

As can be seen from the values of P_{CR} listed above, the minimum P_{CR} occurs at crossection H. Thus the Mach-10 particle separator has a buckling load capability of 7,500 psi.

The last area of the Mach-10 particle separator which merits scrutiny is the flat nose on the front of the separator which is subjected to the dynamic head pressure of 1370 psi acting on a 4 in^2 area.

The shear stress is obtained from Equation (C-1):

$$\tau = \frac{\Delta p\ A_L}{A_S}$$

C-1 Horvay, "The Plane Stress Problem of Perforated Plates," Journal of Applied Mechanics, Vol. 19, 1962.

For the Mach-10 separator,

$\Delta p = q = 1370$ psi

$A_L = 4$ in^2

A_S = (perimeter of loaded area) x (thickness)

= (8) x (.5)

= 4 in^2

Substitution yields

$$\tau = \frac{1480(4)}{(4)} = 1480 \text{ psi}$$

Recall the yield strength of Inconel X-750 is 40,000 psi at 1500°F. The allowable shear is .57 x 40,000, or 22,800 psi, which is much higher than the shear stress obtained above.

To compute bending stresses in the flat nose, the following equation is used:[C-2]

$$\sigma = \frac{3}{2} \frac{\Delta p R^2}{mt^2} \left[m + (m+1) \log \frac{a}{R} - (m-1) \frac{R^2}{4a^2} \right] \qquad \text{(C-7)}$$

where a = plate radius
m = reciprical of Possion's ratio
R = loaded area radius

The equation given above is for simply supported edges. The actual edge condition is somewhere between simply supported and fixed, with the simply supported condition yielding slightly higher stresses.

For the Mach-10 nose:

$R \approx 1"$
$a = 1.4"$
$t = .5"$

$m = 3.3$
$\Delta p = 1370$ psi

[C-2] Roark, R. J., Formulas for Stress and Strain, McGraw-Hill Co., Fourth Edition, 1965.

Substitution into (C-7) yields:

$$\sigma = \frac{3}{2}\frac{1370(1)^2}{3.3(.5)^2}\left[3.3 + (3.3 + 1)\log\frac{1.4}{1} - (3.3 - 1)\frac{1^2}{4(1.4)^2}\right]$$

$$\sigma = 9050 \text{ psi}$$

This value of bending stress is much less than the yield strength of Inconel X-750 at 1500°F (40,000 psi)

MACH-14 SEPARATOR

The Mach-14 separator (Figure C-3) is fabricated from Columbium which has a yield strength of 3000 psi at 3000°F, the Mach-14 gas temperature. An analysis identical to the one used for the Mach-10 separator will be performed for the Mach-14 separator.

The maximum mass flow rate for Mach-14 operations is 130 lb/sec. The density of nitrogen at 20,000 psi and 3000°F is 12 lb/ft^3. The velocity of the gas impinging on the nose of the separator is determined from Equation (C-2):

$$V = \frac{m}{\rho A}$$

Substitution yields

$$V = \frac{130}{12(.028)} = 390 \frac{ft}{sec}$$

The dynamic head pressure associated with this velocity and gas density is, from Equation (C-3).

$$q = \frac{1}{2}\rho V^2 = \frac{1}{2}\frac{12}{32.2}(390)^2$$

$$q = 28{,}340 \frac{lb}{ft^2} = 195 \text{ psi}$$

As in the Mach-10 separator analysis, three crossections (Q, V, Z of Figure C-3) will be analyzed for bearing stresses.

The bearing load due to the 195 psi dynamic head pressure, which is constant for all crossections, is determined from Equation (C-4),

$$F_1 = qA$$

Substitution yields

$$F_1 = 195(4) = 780 \text{ lbs}$$

Equation (C-5) can now be utilized to solve for Δp_{max}. Recall that the yield strength of columbium at 3000°F is 3000 psi. Thus,

$$\Delta p_{max} = \frac{(3000 \cdot A) - 780}{A_e}$$

Values of A, A_E, and Δp_{max} are shown in the table below for the three crossections of interest.

Crossection	A-Crossectional Area (in^2)	A_E-Net Exposed Area (in^2)	P_{max} (psi)
Q	.93	6.25	320
V	2.11	12.35	450
Z	5.30	20.85	725

Thus the maximum pressure drop which the Mach-14 particle separator can tolerate without yielding is the minimum value shown in the table above, or 320 psi.

An estimate will now be made of the external pressure required to buckle the separator. Recall Equation (C-6);

$$P_{CR} = \frac{E}{4(1-\nu^2)} \left(\frac{t}{R}\right)^3$$

Again utilizing the method outlined earlier, the values of E and ν for Columbium are changed to account for the presence of radial holes in the separator. For the Mach-14 particle separator geometry,

$$E^* = .26\ E$$
$$\nu^* = 1.5\ \nu$$

For Columbium at 3000°F, $E = 12.6 \times 10^6$ psi and $\nu = .3$. Thus,

$$E^* = .26\ (12.6 \times 10^6) = 3.3 \times 10^6 \text{ psi}$$

$$\nu^* = 1.5\ (.3) = .45$$

Using E^*, ν^* and the values of t and R given in the table below in Equation (C-6) results in the P_{CR}'s also shown below.

Crossection	t (in)	R (in)	P_{CR} (psi)
Q	.375	1.1	41,000
V	.475	1.6	27,000
Z	.550	2.2	16,000

From the values of P_{CR} listed above it can be seen that the buckling load capability is 16,000 psi based on crossection Z.

Lastly the flat nose of the separator will be analyzed as a plate subjected to the dynamic head pressure q. The shear stress is given by Equation (C-1);

$$\tau = \frac{q\ A_L}{A_S}$$

For a q of 195 psi and the same A_L and A_S as in the Mach-10 case (due to the same plate thickness and load area), the shear stress is

$$\tau = 195\ \frac{(4)}{(4)} = 195\ \text{psi}$$

Recall the yield strength of Columblium at 3000°F is 3000 psi. The allowable shear is thus .57 x 3000, or 1710 psi which is much larger than the value obtained above.

To compute bending stresses Equation (C-7) is employed again. Recall,

$$\sigma = \frac{3}{2}\frac{\Delta p\ R^2}{mt^2}\left[m + (m+1)\log\frac{a}{R} - (m-1)\frac{R^2}{4a^2}\right]$$

For the Mach-14 separator,

$\Delta p = 195$ psi
$R = 1$ in
$a = 1.15$ in

$m = 3.3$

Substitution yields;

$$\sigma = \frac{3}{2}\frac{195\ (1)^2}{3.3\ (.5)^2}\left[3.3 + (4.3 \log \frac{1.15}{1}) - (2.3)\frac{(1)^2}{4(1.15)^2}\right]$$

$$\sigma = 1100 \text{ psi}$$

This value of bending stress is much less than the yield strength of columbium (3000 psi) at 3000°F.

The table below is a summary of the results obtained for the Mach-10 and Mach-14 particle separators.

	Δp_{max} (psi)	P_{CR} (psi)
Mach-10 Separator	1700	7,500
Mach-14 Separator	320	16,000

APPENDIX D

STEADY-STATE PRESSURE DROP CALCULATIONS

To determine the steady-state regime loading condition on the various-heater internals, the pressure drop over the flow path ABCDE shown below must be determined.

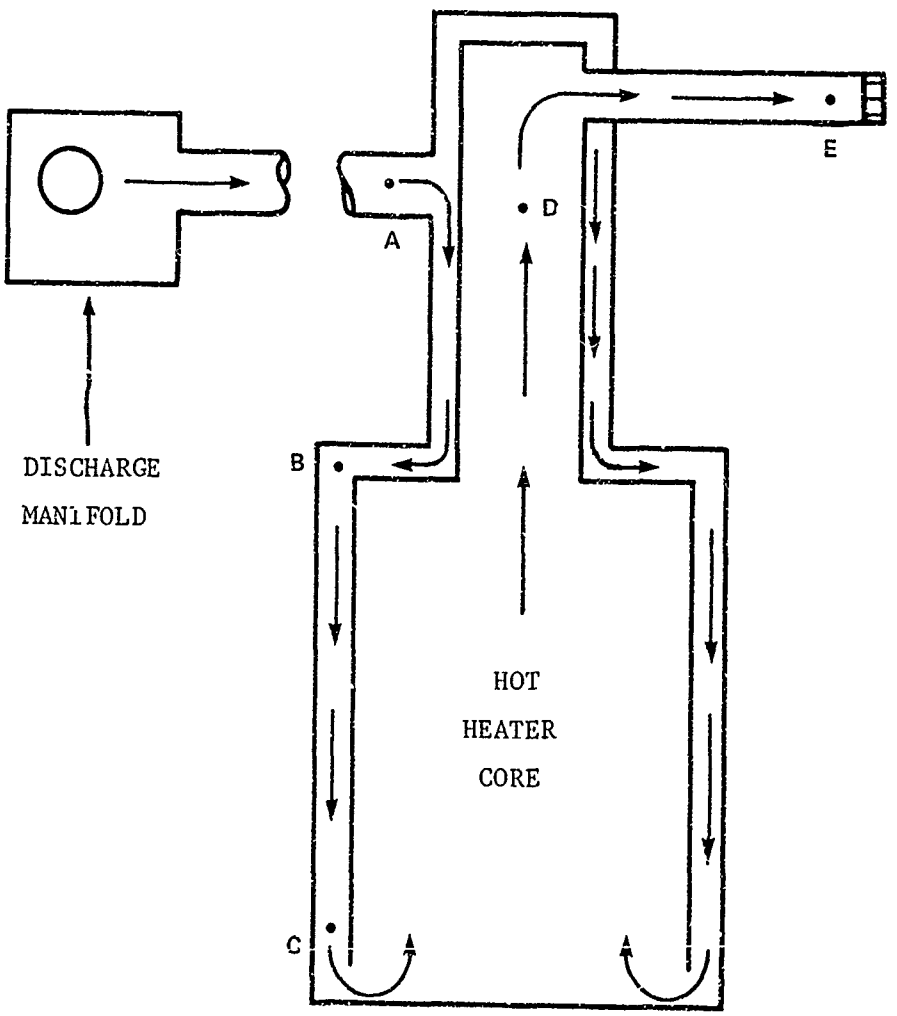

MACH-14 CONDITIONS

The volumetric flow rate throughout the flow passage must be constant. To determine this rate the following equation is used:

$$Q = k_N \, a_H \, A^* \qquad \text{(D-1)}$$

where k_N = nozzle discharge coefficient = .53
a_H = sound speed in the heater gas = 4100 ft/sec
A^* = throat area = .785 in^2 = .00545 ft^2

Substitution yields:

$$Q = .53 \; (4100) \; (.00545)$$

$$Q = 11.8 \; ft^3/sec = \text{constant}$$

To determine the mass flow rate in any section, the following relation is used;

$$m = \rho \cdot Q \qquad \text{(D-2)}$$

where ρ = density of gas at a particular section

Now the various pressure drops will be computed. Due to the high densities involved, a fluid flow approach is taken.

First, obtain the pressure drop through the vertical elbow, Δ_{pA-B}. The gas flowing from the driver vessels is at 300°F. The density of nitrogen at 300°F and 22,000 psi is 39 lb/ft^3.

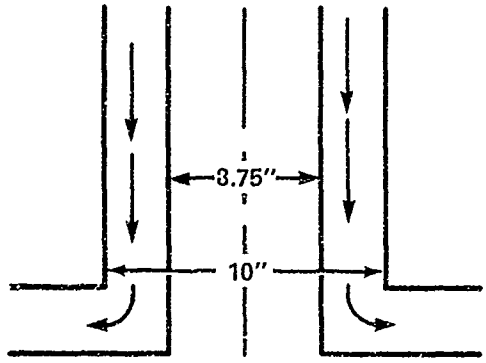

The gas velocity in the vertical elbow annular gap is determined from;

$$V = \frac{Q}{A} \qquad \text{(D-3)}$$

where A = crossectional area

$$= \left[10^2 - 8.75^2\right] \frac{\pi}{4}$$

$$= 18.4 \text{ in}^2 = .128 \text{ ft}^2$$

Thus

$$V = \frac{11.8}{.128} = 92.3 \text{ ft/sec}$$

The dynamic head pressure, "q" is obtained from

$$q = \frac{1}{2} \frac{\rho v^2}{g} \qquad \text{(D-4)}$$

Substitution yields

$$q = \frac{1}{2} (39) \frac{1}{32.2} (92.3)^2$$

$$q = 5155.2 \text{ lb/ft}^2 = 35.8 \text{ psi}$$

The Reynolds number must be otained to determine the friction factor.

$$R_e = \frac{VD_e\rho}{\mu} \qquad \text{(D-5)}$$

where D_E = Equivalent diameter = $\frac{(10 - 8.75)}{12}$

D_E = .104 ft
μ = viscosity of nitrogen at 300°F and 22,000 psi
μ = .14 lb/hr-ft

Substitution into Equation (D-5) yields:

$$R_e = \frac{92.3(.104)(39)}{.14} (3600 \text{ sec/hr})$$

$$R_e = 9.6 \times 10^6/\text{ft}$$

The pressure drop is obtained from

$$\Delta p = 4f \frac{L}{D_e} \cdot q \qquad \text{(D-6)}$$

where f = friction factor based on wall roughness and Reynolds No.
L = length of section = 3.5 ft

The friction factor "f" is obtained from the Moody diagram.[D-1] For an $R_e = 9.6 \times 10^6$ and commercial steel wall roughness, an f = .0055 was obtained. Substitution into Equation (D-6) yields.

$$\Delta p_{A-B} = 4(.0055)\frac{(3.5)}{(.104)}(35.8)$$

$$\Delta p_{A-B} = 26.5 \text{ psi}$$

In a similar fashion the pressure drop from B to C is calculated. The gas density remains 39 lb/ft^3. The gas velocity, from (D-3) is:

$$V = \frac{Q}{A}$$

$$= \frac{11.8}{[24^2 - 23.5^2]\frac{\pi}{4}} \times 144 \frac{in^2}{ft^2}$$

$$V = 90.8 \text{ ft/sec}$$

The dynamic head pressure, from (D-4) is:

$$q = \frac{1}{2}\frac{p}{g}V^2 = \frac{1}{2}\frac{(39)}{32.2}\frac{90.8^2}{144}$$

$$q = 34.7 \text{ psi}$$

The Reynolds number, obtained from (D-5) is

$$R_e = \frac{V D_e \rho}{\mu} = 90.8 \frac{\left(\frac{24 - 23.5}{12}\right) 39 \times 3600}{.14}$$

$$R_e = 3.8 \times 10^6/\text{ft}$$

The friction factor "f" from the moody diagram is .0065.

[D-1] Streeter, V. L., Fluid Mechanics, McGraw-Hill Book Co., Fifth Edition, 1971.

Finally the pressure drop from B to C, using equation (D-6) is:

$$\Delta p_{B-C} = 4f \frac{L}{D_e} q$$

$$= 4\ (.0065)\ \frac{(9.2)}{(.0417)}\ 34.7$$

$$\Delta p_{B-C} = 199 \text{ psi}$$

The pressure drop from C to E is negligible due to the low gas velocity through the main heater section.

An estimate of the turning losses can be made from the following:

$$\Delta p_{turns} = kq \qquad \text{(D-7)}$$

where k is a factor based on the type of turn encountered,
q = dynamic head pressure

For a 90° turn, k = 1.13. There are 3-90° turns in the flow path A-D, thus:

$$\Delta p_{turns} = 3\ (k)\ q$$

Substitution yields

$$\Delta p_{turns} = 1.13\ (3)\ (35) \text{ psi} = 118.7 \text{ psi}$$

The total pressure drop over the flow path A-E is then;

$$\Delta P_{A-E} = \Delta P_{A-B} + \Delta P_{B-C} + \Delta P_{C-E} + \Delta P_{turns} \qquad \text{(D-8)}$$

$$= 26.5 + 199 + 0 + 118.7$$

$$\Delta p_{A-E} = 344.2 \text{ psi}$$

MACH-10 CONDITIONS

The geometry of the flow path ABCDE is the same as the geometry for Mach-14 operating conditions. The heater gas temperature is now 1500°.

Recall Equation (D-1) to determine the volumetric flow rate,

$$Q = k_N\ a_H\ A^*$$

For Mach-10 conditions,

$k_N = .53$
$A_H = 3200$ ft/sec

For Mach-10 operation, the flow restrictor acts as a first throat. Thus;

$$A^* = 7\ (.46^2)\ (\frac{\pi}{4}) = 1.163 in^2 = .0081 ft^2$$

Substitution into Equation (D-1) yields,

$$Q = .53\ (3200)\ (.0081)$$

$$Q = 13.74\ ft^3/sec$$

As in the Mach-14 case, the pressure drop across various sections of the flow passage will now be determined. As before, first obtain the pressure drop through the vertical elbow, Δ_{PA-B}.

The gas flowing from the driver vessels is at 300°F. The density of nitrogen at 300°F and 22,000 psi is 39 lb/ft^3. The gas velocity in the elbow section is determined from Equation (D-3);

$$V = \frac{Q}{A}$$

Substitution yields

$$V = \frac{13.74}{.128} = 107.3\ \frac{ft}{sec}$$

The dynamic head pressure, from Equation (D-4) is then,

$$q = \frac{1}{2}\frac{\rho}{g} V^2$$

$$q = \frac{1}{2}\frac{39}{32.2}\ (107.3)^2$$

$$q = 6972\ lb/ft^2 = 48.4\ psi$$

The Reynolds nunber is obtained by use of Equation (D-5);

$$R_e = \frac{V\ D_e \rho}{\mu}$$

$$R_e = \frac{(107.3)\ (.104)\ (39)}{.14}\ 3600\ \frac{sec}{hr}$$

$$R_e = 11.2 \times 10^6/ft$$

The pressure drop through the elbow section is now obtained from Equation (D-6);

$$\Delta p = 4f \frac{L}{D_e} q$$

For a Reynolds number of 11.2 x 10^6/ft and commercial steel wall roughness, a friction factor of .00575 is obtained. Substitution into (D-6) yields;

$$\Delta p_{A-B} = 4(.00575) \frac{(3.5)}{(.104)} (48.4)$$

$$\Delta p_{A-B} = 37.5 \text{ psi}$$

The pressure drop from B to C will now be obtained. The gas density remains 39 lb/ft^3 due to the gas temperature and pressure remaining close to 300°F and 22,000 psi respectively.

The gas velocity in section C is, from Equation (D-3),

$$V = \frac{Q}{A} = \frac{13.74}{.13}$$

$$V = 105.7 \text{ ft/sec}$$

The dynamic head pressure, from Equation (D-4) is,

$$q = \frac{1}{2} \frac{\rho}{q} V^2 = \frac{1}{2} \cdot \frac{39}{32.2} \left(105.7\right)^2$$

$$q = 6766 \text{ lb/ft}^2 = 47 \text{ psi}$$

The Reynolds number, obtained from Equation (D-5) is,

$$R_e = \frac{V D_e \rho}{\mu} = \frac{105.7 (.0417) (39)}{.14} \times 3600$$

$$R_e = 4.4 \times 10^6/\text{ft}$$

The friction factor for this Reynolds number is from Reference D-1, .00525. The pressure drop from B to C is thus found, using Equation (D-6),

$$\Delta p = 4f \frac{L}{D} 9 = 4(.00525) \frac{(9.2)}{(.0417)} 47$$

$$\Delta p = 218 \text{ psi}$$

As in the Mach-14 case, the pressure drop from C to E is negligible due to the low gas velocities involved.

D-1 See footnote D-1 on page D-4.

An estimate of the turning losses is made using Equation (D-7),

$$\Delta p_{turns} = (\text{number of turns})\ (k)\ (q)$$

$$\Delta p_{turns} = 3\ (1.13)\ (48)$$

$$\Delta p_{turns} = 162.7 \text{ psi}$$

The total pressure drop oven path ABCDE is then,

$$\Delta p_{A-E} = \Delta p_{A-B} + \Delta p_{C-E} + \Delta p_{turns}$$

$$\Delta p_{A-E} = 37.5 + 218 + 0 + 162.7$$

$$\Delta p_{A-E} = 418.2 \text{ psi}$$

The table below summarizes the results obtained for both Mach-10 and Mach-14 conditions

	Δp_{A-B}	Δp_{B-C}	Δp_{Turns}	Δp_{Total}
Mach-10	37.5	218	162.7	418.2
Mach-14	26.5	199	118.7	344.2

APPENDIX E

MACH-10 VS MACH-14 DEPRESSURIZATION RATES

From continuity considerations, the flow rate through the heater is equal to the flow rate through the flow restrictor. In equation form;

$$m = \rho_H u A_H = K_N \rho_R a_R A_R \tag{E-1}$$

where the subscripts H and R refer to heater and restrictor area respectively. Solving for u, the velocity of the rarefaction wave, the following is obtained;

$$u = \frac{k_N \rho_R a_R A_R}{\rho_H A_H} \tag{E-2}$$

Recall now Equation (1) from the main report:

$$\Delta p = \rho_H a_H U \tag{E-3}$$

Substitution of Equation (E-2) into Equation (E-3) yields:

$$\Delta p = k_N \rho_R a_R \frac{A_R}{A_H} a_H \tag{E-4}$$

It can be seen from the above equation then, that for a given geometry (A_R/A_H) and a given flow restrictor condition ($k_N \rho_R a_R$), Δp is proportional to a_H, the sound speed in the heater. Both Mach-10 and Mach-14 utilize the same geometry, and during the transient period, cold gas is moving through the flow restrictor area in both Mach-10 and Mach-14 operations. Thus, it can be written;

$$\frac{\Delta p_{M-10}}{\Delta p_{M-14}} = \frac{a_{H10}}{a_{H14}} \tag{E-5}$$

The sound speed may be determined from;

$$a = \sqrt{\frac{\gamma P}{\rho}} \tag{E-6}$$

But for Mach-10 and Mach-14 operations, p is the same. Substitution of Equation (E-6) into (E-5), and elmination of p results in the following;

$$\frac{\Delta p_{M-10}}{\Delta p_{M-14}} = \frac{\left(\frac{\gamma}{\rho}\right)10}{\left(\frac{\gamma}{\rho}\right)14} \qquad \text{(E-7)}$$

For nitrogen at 1500°F (Mach-10), γ = 1.95 and ρ = 19.5 lb/ft^3. For nitrogen at 3000°F (Mach-14), γ = 1.61, and ρ = 12.7 lb/ft^3. Substitution into Equation (E-7) yields;

$$\frac{\Delta p_{M-10}}{\Delta p_{M-14}} = \sqrt{\frac{\frac{1.95}{19.5}}{\frac{1.61}{12.7}}} = .89$$

Thus the magnitude of the rarefaction wave strength in Mach-10 is about 90% of the Mach-14 value.

Such is not the case for the depressurization occurring at the end of a run, when the control valves shut. The depressurization of the heater is calculated from;

$$\frac{1}{P_H}\frac{dp}{dt} = -\frac{\gamma_{EFF} k_N a_H A^*}{V_H} \qquad \text{(E-8)}$$

where V_H = Heater Volume

γ_{eff} is determined from;

$$\gamma_{EFF} = \frac{V_H}{\frac{V_{HOT}}{\gamma_{HOT}} + \frac{V_{COLD}}{\gamma_{COLD}}}$$

Now relating the Mach-10 situation to Mach-14 by use of Equation (E-8);

$$\frac{\left(\frac{1}{P_H}\frac{dp}{dt}\right)_{M-10}}{\left(\frac{1}{P_H}\frac{dp}{dt}\right)_{M-14}} = \frac{\left(\gamma_{EFF}\right)_{M-10}}{\left(\gamma_{EFF}\right)_{M-14}} \frac{a_{H\ M-10}}{a_{H\ M-14}}$$

Recall though, that $(a_{H\ M-10})/(a_{H\ M-14})$ was previously determined to be .9. γ_{EFF} for Mach-10 and Mach-14 conditions must be determined.

V_H, V_{HOT}, and V_{COLD} are the same for Mach-10 and Mach-14 due to similar heater geometry. V_H is 26 ft^3, V_{HOT} is 22 ft^3 and V_{COLD} is 4 ft^3. The table below contains values of γ_{HOT}, γ_{COLD} and γ_{EFF} for both Mach-10 and Mach-14 conditions.

DISTRIBUTION

	Copies
Commander	
Naval Sea Systems Command	
Attn: SEA 09G32	2
SEA 03B	1
Washington, DC 20362	
Office of Naval Research	
800 N. Quincy Street	
Arlington, VA 22217	2
Office of Chief of Naval Operations	
Operation Evaluation Group	
Washington, DC 20350	1
Library of Congress	
Attn: Gift and Exchange Division	4
Washington, DC 20540	
Defense Nuclear Agency	
Washington, DC 20301	2
Headquarters	
Air Force Special Communications Center	
USAFSS San Antonio, TX 78243	1
Defense Tech Information Center	
Cameron Station	
Alexandria, VA 22314	12
Internal Distribution:	
Bellamy (K22)	1
Brown (K22)	
Brunsvold (K22)	1
Dorsey (K22)	1
Edwards (K22)	1
Etheridge (K22)	1
Gorechlad (K22)	1
Hannah (K22)	1
Jones (K22)	1
Messick (K22)	1
Morrison (K22)	1
Mungiole (K22)	1
Rees (K22)	1
Regan (K22)	1
Vamos (K22)	1
Cornett (K23)	1
Kavetsky (K23)	1
Metzger (K23)	1
Mitchell (K23)	1
Rozanski (K23)	1
Schlie (K23)	1
Waser (K23)	1
Waldo (K23)	1
Ausherman (K24)	1
Baltakis (K24)	1
Bell (K24)	1
Cothran (K24)	1
Driftmyer (K24)	1
Falusi (K24)	1
Fiscina (K24)	1
Gorney (K24)	1
Hawkins (K24)	1
Hill (K24)	1
Jobe (K24)	1
King (K24)	1
Knott (K24)	1
Krumins (K24)	1
Prats (K24)	1
Ragsdale (K24)	1
Roberts (K24)	1
Sheetz (K24)	1
Voisinet (K24)	1
Watts (K24)	1
Westermeyer (K24)	1
Yanta (K24)	1
K20	1
K	1
E431	9
E432	3
E35	1